An update on the recent advances and discovery of novel tubulin colchicine binding inhibitors

Haoxiang Weng[†], Jinlong Li[†], Huajian Zhu[†*], Kei Fung Carver Wong[‡], Zheying Zhu[‡], Jinyi Xu[†*]

[†]State Key Laboratory of Natural Medicines & Department of Medicinal Chemistry, China Pharmaceutical University, 24 Tong Jia Xiang, Nanjing 210009, PR China

[‡]School of Pharmacy, The University of Nottingham, University Park Campus, Nottingham NG7 2RD, UK

*Author for correspondence: jinyixu@china.com (J. Xu.) ; cpuzhj@126.com (H. Zhu.)

Jinyi Xu* ORCID: 0000-0002-1961-0402

Graphical abstract:

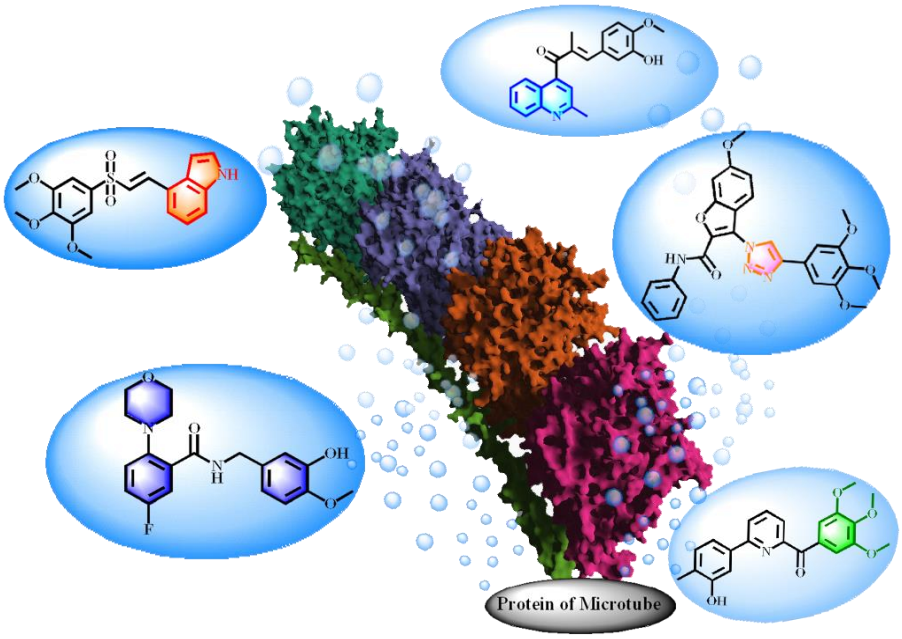

Abstract: Microtubules, formed by α- and β-tubulin heterodimer, are considered as a major target to prevent the proliferation of tumor cells. Microtubule-targeted agents (MTAs) have become increasingly effective anticancer drugs. However, due to the relatively sophisticated chemical structure of taxane and vinblastine, the application of them has faced numerous obstacles. Conversely, the structure of colchicine binding site inhibitors (CBSIs) is much easier to be modified. Moreover, CBSIs have strong antiproliferative effect on multidrug resistant tumor cells and have become the mainstream research orientation of MTAs. This review mainly focuses on the recent advances of CBSIs during 2017-2022, attempts to depict their biological activities to analyze the structure activity relationships (SARs), and offers new perspectives for designing next generation of novel CBSIs.

Keyword: tubulin polymerization inhibitors, colchicine binding site, antiproliferative effect, structure modification, SARs

1. Introduction

Cancer has been one of the largest worldwide risks to human mortality every year, and lung cancer has become the leading cause of death among cancers and the incidence of breast and prostate cancers gradually increased in the last decade [1-2]. The overall risk of cancer is on the decline due to advances in early diagnostic techniques, surgical equipment and targeted therapies, which is undoubtedly a good prospect, but the effective treatment for all types of cancer remains a difficult problem. Scientists continue to explore and design new effective pharmaceuticals specifically targeting tumor cells with low or even no toxicity to normal cells. Microtubules, a critical component of eukaryotic cells, are hollow cylinders formed by the polymerization of α-tubulin and β-tubulin heterodimers (Fig. 1), which play an important role in the formation of the cell cytoskeleton, maintenance of cell morphology, signal transduction and mitosis [3-6]. Microtubules are also involved in the growth, proliferation and migration of cancer cells, and form the framework of tumor endothelial vascular cells, thus allowing them to continuously acquire nutritional supplies through angiogenesis [7]. Thus, microtubules are considered as one of the most important key targets for the development of anti-cancer drugs. Microtubule-targeted inhibitors can effectively disrupt the kinetic process of microtubules, further interfere with the mitotic process and the formation of the spindle, block the cell cycle at the middle or late phases of mitosis, and finally induce apoptosis [8-9]. Microtubule-targeted agents (MTAs) are currently one of the key orientations in anti-tumor research and development. MTAs can act precisely on microtubule proteins, and the microtubule dynamic system of tumor cells is generally more active because of their rapid proliferation. Thus MTAs are more sensitive towards tumour cells than normal cells, leading to reduced toxicity towards normal cells and improving the therapeutic effect [10]. MTAs are divided into microtubule aggregation inhibitors (e.g. those targeting colchicine and vincristine-binding sites) and inhibitors of microtubule depolymerisation (e.g. those targeting paclitaxel binding sites) [11-13]. The disadvantages of paclitaxel and vincristine hinder them to be the first choice of anti-cancer drugs: (1) the difficulty in achieving industrial standard production of the compound by total synthesis methods due to the relatively complex chemical structures; (2) the low yield of raw material extraction; (3) the difficulty in structure modification; (4) the dose toxicity and drug resistance in clinical applications. In contrast, colchicine binding site was identified at the interface between α-tubulin and β-tubulin (Fig. 1), which would significantly change conformation in the transition from the unpolymerized to the polymerized state in the previous study [14]. Therefore, colchicine binding site inhibitors (CBSIs) could have potent interactions in the binding site leading to the stagnation of microtubule polymerization. CBSIs researches have yielded fruitful results since these agents are more easily modified and have a strong anti-proliferative effect on multidrug resistant (MDR) cancer cells, which has aroused a great deal of interest among researchers. There were several representative compounds of microtubule inhibitors approved by FDA or reaching clinical trials such as Ixabepilone (approved), Eribulin

(approved), Monomethyl Auristatin E (approved), Plinabulin (NCT02846792), Indibulin (NCT00591136), CA-4P (NCT01570790), Oxi4503 (NCT00977210), KX2-361 (NCT02326441) and ABT-751 (NCT00073138; NCT00073151), etc [15-19]. In addition, there are some other effective backbones under research, which we will introduce as follows.

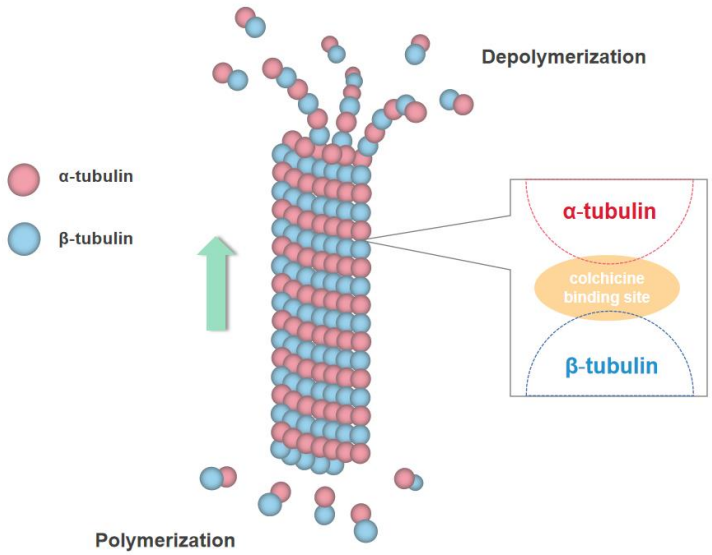

Fig. 1 Microtubule dynamics and location of colchicine binding site

2. Development of molecules as colchicine binding site inhibitors

2.1. The structure-activity relationship and anti-tumor activities of the derivatives containing indole and its analogue backbone

Various derivatives based on the indole backbone have the biological effect of anti-inflammatory, anti-hypertensive and anti-cancer properties. Multitudes of natural and artificial molecules with indole structure have been discovered with the perseverance of researchers and many of them have been reported as microtubule inhibitors in the last five years. Sravanthi *et al* designed and synthesized a series of pyrimidine-5-aminoindole derivatives and evaluated the antiproliferative activities of them against DU145, PC-3, A549 and HCT-15 cancer cells [20]. The best antiproliferative activity was discovered for the para-substituted chlorine compound **1** and para-substituted fluorine compound **2** (Fig. 2) against human prostate cancer cells (DU145) with IC_{50} values of 140 nM and 180 nM, respectively. The optimal compound **1** substituted with chlorine also showed high antiproliferative activity to PC-3 and HCT-15 cells (IC_{50} = 220 nM, 260 nM, respectively). According to the analysis of structure activity relationship (SAR) of these compounds, an electron-withdrawing group introduced at the para-position of the benzene ring was able to increase the antiproliferative activity significantly and when the 4-position was substituted with an electron-donating group such as methyl or methoxy, the antiproliferative activity decreased. Furthermore, the antiproliferative activity disappeared when there was only the benzene ring. The conclusion is that the introduction of electron-withdrawing groups at the 4-position of the benzene ring connected to pyrimidine can significantly improve the antiproliferative activity *in vitro*.

Mirzaei *et al* designed and synthesized some indole-chalcone derivatives and evaluated their antiproliferative activity against various cancer cells [21]. Among them, compound **3** (Fig. 2) with 3-bromo-4,5-dimethoxybenzene structure showed good antiproliferative activity against A549 cells (IC_{50} = 4.3 μg/mL), which was more effective than the positive control (IC_{50} = 7.8 μg/mL). The SAR showed that the anticancer effect was lessened when the 3,4,5-trimethoxybenzyl ring was combined in the compound through a linkage on the 3-position of indole ring. The results suggested that the 3-bromo-4,5-dimethoxybenzyl ring played an important role in the antiproliferative activity. In addition, compound **3** inhibited microtubule aggregation and reduced thiol content in mitochondrion to induce apoptosis in tumor cells. Molecular docking analysis showed that compound **3** has perfectly docking in the colchicine binding site through hydrophobic interactions with residues Ala180, Asn249, Ala354, and Leu248, etc. The carbonyl group has strong hydrogen bond interactions with the residues, such as Asp251, Leu252 and Leu255. The bromine atom has the halogen interaction with the residues Lys352 and Ala317. In another report, Wang *et al* designed and synthesized a series of new naphthalene ring indole ketone derivatives [22]. According to the SAR, the attachment of a bulk steric group on the N-1 position of indole ring would lead to a decreased antiproliferative effect. The antiproliferative activity was significantly lower when substituted by benzyl or other bulky alkyl groups, and the activity was optimal when a small methyl group was attached. Moreover, the compound was more active when *α,β*-unsaturated ketone was attached at the C-5 position of the indole benzene ring than at any other position, and had the weakest effect when attached at the C-7 position. Therefore, considering comprehensively, the optimal compound **4** (Fig. 2) with the methyl group attached N-1 position and the *α,β*-unsaturated ketone at the C-5 position showed the best antiproliferative activity with IC_{50} values of 0.82 μM, 1.13 μM and 0.65 μM against three tumor cells (MCF-7, HCT116 and HepG2), respectively. Kode *et al* designed and synthesized a series of trimethoxyphenyl indole chalcone derivatives and conducted *in vitro* cell biological tests [23]. Compound **5** (Fig. 2), in which the indole *N*-1 methyl substituent and the other end of the benzene ring R^1 and R^2 were methoxy groups, showed excellent antiproliferative activity against oral cancer squamous cells (SCC-29B) with GI_{50} value less than 0.1 μM. When R^1 and R^2 of the benzene ring was replaced by chlorine atoms (compound **6**), it showed good antiproliferative activity against colon cancer cells (HT-29) (GI_{50} < 0.1 μM). When R^2 methoxy group was replaced by electron-withdrawing group such as nitro group like compound **7** was yielded, which was highly lethal to HepG2 cells with GI_{50} value of only 18 nM. *In vitro* kinetic analysis of microtubule polymerization showed that compound **6** interacted directly with tubulin, inhibiting tubulin polymerization and leading to the production of unstable tubulin intermediates.

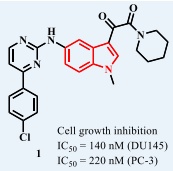

1

Cell growth inhibition
IC_{50} = 140 nM (DU145)
IC_{50} = 220 nM (PC-3)
IC_{50} = 260 nM (HCT-15)
IC_{50} = 1.2 μM (A549)
Tubulin polymerization inhibition
IC_{50} = 0.40 μM

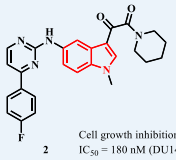

2

Cell growth inhibition
IC_{50} = 180 nM (DU145)
IC_{50} = 2.8 μM (PC-3)
IC_{50} = 3.2 μM (HCT-15)
IC_{50} = 1.6 μM (A549)

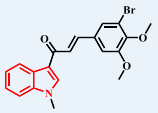

3

IC_{50} = 4.3 μg/ mL (A549)
Tubulin polymerization inhibition
IC_{50} = 17.8 μM

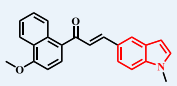

4

Cell growth inhibition
IC_{50} = 0.82 μM (MCF-7)
IC_{50} = 1.13 μM (HCT-116)
IC_{50} = 0.65 μM (HepG2)
Tubulin polymerization inhibition
IC_{50} = 3.9 μM

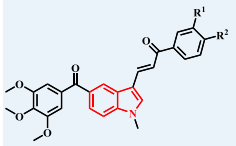

5: R^1, R^2 = OCH_3
6: R^1, R^2 = Cl
7: R^1 = H, R^2 = NO_2

Cell growth inhibition
GI_{50} < 0.1 μM (SCC-29B)
GI_{50} < 0.1 μM (HT-29)
GI_{50} = 18 nM (HepG2)

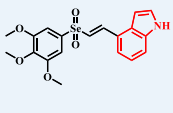

8

Cell growth inhibition
IC_{50} = 0.287 μM (K562)
IC_{50} = 0.525 μM (HepG2)
IC_{50} = 0.621 μM (HCT-8)
Tubulin polymerization inhibition
IC_{50} = 1.82 μM

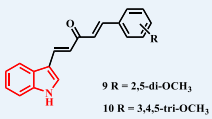

9 R = 2,5-di-OCH_3
10 R = 3,4,5-tri-OCH_3

Cell growth inhibition
9 IC_{50} = 6.34 μM (PC-3)
IC_{50} = 6.59 μM (Hela)
10 IC_{50} = 3.15 μM (PC-3)
IC_{50} = 3.31 μM (Hela)

Tubulin polymerization inhibition
IC_{50} = 10.23 μM
IC_{50} = 8.81 μM

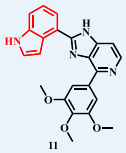

11

Cell growth inhibition
IC_{50} = 7.6 nM (A375)
IC_{50} = 9.6 nM (SK-MEL-1)
IC_{50} = 10.1 nM (RPMI7951)
IC_{50} = 10.3 nM (WM115)
colchicine
IC_{50} = 9.1 nM (A375)
IC_{50} = 9.0 nM (SK-MEL-1)
IC_{50} = 8.3 nM (RPMI7951)
IC_{50} = 8.2 nM (WM115)

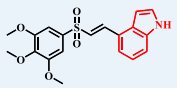

12

Cell growth inhibition
IC_{50} = 75 nM (HepG2)
IC_{50} = 305 nM (A549)
IC_{50} = 55 nM (K562)
IC_{50} = 80 nM (Bel-7402)
IC_{50} = 60 nM (H22)
Tubulin polymerization inhibition
IC_{50} = 3.09 μM

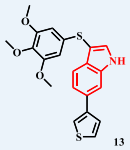

13

Cell growth inhibition
IC_{50} = 4.5 nM (MCF-7)
IC_{50} = 10 nM (HT29)
IC_{50} = 21 nM (HCT116)
IC_{50} = 6 nM (MV4-11)
IC_{50} = 2 nM (A549)
Tubulin polymerization inhibition
IC_{50} = 0.58 μM

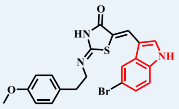

14

Cell growth inhibition
IC_{50} = 0.92 μM (HCT-15)
IC_{50} = 2.802 μM (HCT-29)
Tubulin polymerization inhibition
IC_{50} = 2.92 μM

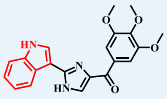

ABI-231

Cell growth inhibition
IC_{50} = 7.2 nM (WM164)
IC_{50} = 8.1 nM (A375)
IC_{50} = 5.6 nM (M14)

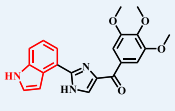

15

Cell growth inhibition
IC_{50} = 1.6 nM (WM164)
IC_{50} = 3.6 nM (A375)
IC_{50} = 3.7 nM (M14)

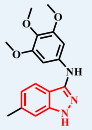

16

Cell growth inhibition
GI_{50} = 15 nM (HCT-116)
GI_{50} = 27 nM (HepG2)
GI_{50} = 33 nM (A549)

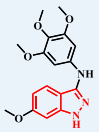

17

Cell growth inhibition
GI_{50} = 41 nM (HCT-116)
GI_{50} = 53 nM (HepG2)
GI_{50} = 65 nM (A549)

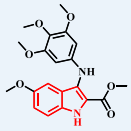

18

Cell growth inhibition
IC_{50} = 0.50 μM (HeLa)
IC_{50} = 0.96 μM (HT29)
IC_{50} = 0.50 μM (MCF-7)
IC_{50} = 1.4 μM (HL-60)
Tubulin polymerization inhibition
IC_{50} = 0.40 μM

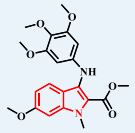

19

Cell growth inhibition
IC_{50} = 0.54 μM (HeLa)
IC_{50} = 0.32 μM (HT29)
IC_{50} = 0.11 μM (MCF-7)
IC_{50} = 1.1 μM (HL-60)
Tubulin polymerization inhibition
IC_{50} = 0.37 μM

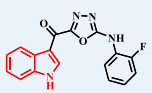

20

Cell growth inhibition
IC_{50} = 2.42 μM (MCF-7)
Tubulin polymerization inhibition
IC_{50} = 3.89 μM

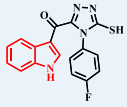

21

Cell growth inhibition
IC_{50} = 3.06 μM (MCF-7)
Tubulin polymerization inhibition
IC_{50} = 8.32 μM

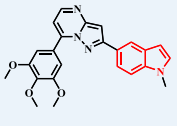

22

Cell growth inhibition
IC_{50} = 19 nM (Hela)
IC_{50} = 3 nM (MCF-7)
IC_{50} = 15 nM (A549)
IC_{50} = 39 nM (HCT-116)
IC_{50} = 48 nM (B16-F10)
Tubulin polymerization inhibition
IC_{50} = 6.7 μM

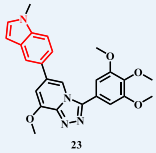

23

Cell growth inhibition
IC_{50} = 15 nM (HeLa)
IC_{50} = 69 nM (A549)
IC_{50} = 49 nM (MCF-7)
IC_{50} = 33 nM (HCT116)
Tubulin polymerization inhibition
IC_{50} = 1.64 μM

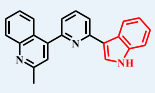

24

Cell growth inhibition
IC_{50} = 4.5 nM (K562)
IC_{50} = 8 nM (A549)
IC_{50} = 10.1nM (MCF-7)
IC_{50} = 2.2 nM (HCT116)
IC_{50} = 3.6 nM (MiaPaca2)

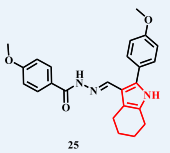

25

Cell growth inhibition
IC_{50} = 1.77 μM (MCF-7)
IC_{50} = 3.75 μM (A549)

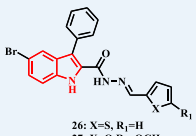

26: X=S, R_1=H
27: X=O,R_1=OCH_3

Cell growth inhibition
26 IC_{50} = 0.19 μM (A549) IC_{50} = 3.6 μM (HUCCA-1)
IC_{50} = 0.07 μM (MOLT-3) IC_{50} = 0.73 μM (HepG2)
27 IC_{50} = 0.06 μM (A549) IC_{50} = 47.4 μM (HUCCA-1)
IC_{50} = 0.09 μM (MOLT-3) IC_{50} = 0.34 μM (HepG2)

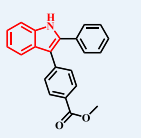

28

Cell growth inhibition
IC_{50} = 5.17 μM (A549)

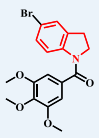

29

Cell growth inhibition
IC_{50} = 1.84 μM (MGC-803)
IC_{50} = 6.82 μM (A549)
IC_{50} = 1.61 μM (Kyse30)

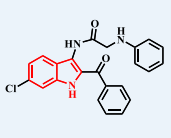

30

Cell growth inhibition
IC_{50} = 15.41 μM (HeLa)
IC_{50} = 11.99 μM (HCT116)
IC_{50} = 14.43 μM (PC-3)

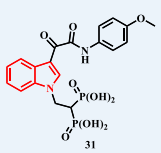

31

Cell growth inhibition
IC_{50} = 0.034 μM (A375)
IC_{50} = 0.223 μM (A549)
IC_{50} = 0.222 μM (HST116)
IC_{50} = 0.478 μM (DU145)
IC_{50} = 0.658 μM (T47D)

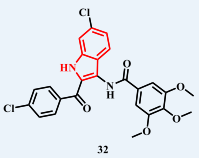

32

Cell growth inhibition
IC_{50} = 6.43 μM (MDA-MB-231)
IC_{50} = 3.17 μM (BT549)
IC_{50} = 0.04 μM (T47D)

Fig. 2 Chemical structures of compounds **1**~**32**

A series of novel vinyl selenone derivatives were designed and synthesized by Zhu *et al* in our research group [24]. Among them, compound **8** (Fig. 2) with vinyl selenone linked indole C-4 position has the best antiproliferative activity against K562, HepG2 and HCT-8 cells, with IC_{50} of 0.287 μM, 0.525 μM and 0.621 μM respectively. SAR analysis showed that the antiproliferative activity was reduced by the substitution of the methyl group at the 1-position. C-4 position of indole linked vinyl selenone was better than other positions. Further studies showed that compound **8** could inhibit tubulin aggregation with IC_{50} value of 1.82 μM. Immunofluorescence analysis suggested that the compound **8** could effectively disrupt the microtubule network of K562 cells in a dose-dependent manner. As reported by Ramya *et al*, a series of derivatives containing indole chalcone were designed and tested for their antiproliferative activity against eight kinds of cells (A549, MDA-MB-231, BT549, 4T1, PC-3, DU145, HGC-27 and HeLa) [25]. SAR analysis indicated that when the para-position of benzene was substituted by an electron-withdrawing group, the compound had weak antiproliferative activity against HeLa, 4T1 and BT549 cells. However, there are electron-donating groups on the benzene (2,5-dimethoxy or 3,4,5-trimethoxy like compound **9** or **10**) (Fig. 2), the derivatives showed moderate antiproliferative activity on PC-3 and HeLa cells, with IC_{50} from 3.15 μM to 6.59 μM. The results suggested that the introduction of electron-donating groups on the benzene of this series of compounds was beneficial for enhancing the antiproliferative activity. Further studies showed that compounds **9** and **10** bound to the colchicine binding site of tubulin, inhibiting microtubulin aggregation and interfering with the cell mitochondrial membrane potential. In the work reported in 2018, Arnst *et al* discovered a series of indole-imidazole compounds and evaluated the antiproliferative activity against four tumor cells (A375, RPMI-7951, WM115 and SK-MEL-1) [26]. The results showed that the antiproliferative activity of compound **11** was potent in tumor cells and the IC_{50} values ranged from 7.6 nM to 10.3 nM, which was almost the same as that of the colchicine. Compound **11** (Fig. 2) significantly inhibited tumor growth in nude mice of A375 transplanted tumor model and completely inhibited the growth of prostate tumor in paclitaxel resistant transplanted tumor model nude mice. For the research in our group, wenlong Li designed and synthesized twenty-two new indole-vinyl sulfone derivatives as tubulin polymerization inhibitors [27]. Among them, compound **12** (Fig. 2) showed the strongest cytotoxicity to three cancer cells (HepG2, A549 and K562), with IC_{50} values of 75 nM, 305 nM and 55 nM respectively. Further research showed that compound **12** effectively disrupted the microtubule network of K562 cells which led to cell cycle arrest in G2/M phase and induced apoptosis. In addition, compound **12** reduced the migration of HUVEC cells and prevented the formation of capillaries. The SAR indicated that the antiproliferative activity was enhanced when the C-4 position of indole ring was substituted. In contrast, when the indole ring was replaced by a pyridine or pyrrole ring, the antiproliferative activity of the compound disappeared. Importantly, compound **12** showed good anti-tumor activity *in vivo* on H22 liver cancer transplanted tumor

model in nude mice with reduced tumor weights of 63.6%. Molecular docking showed that compound **12** interacted with tubulin at the colchicine binding site.

Regina *et al* designed and identified novel 3-arylthio- and 3-aroyl-1*H*-indole derivatives [28]. According to SAR, the presence of thiophene heterocycle at position 6 or 7 of the indole section could enhance the antiproliferative activity and strongly inhibited both tubulin polymerization and the growth of MCF-7 cancer cells. Compound **13** (Fig. 2) reached an IC_{50} value of 4.5 nM, and inhibited a group of cancer cells and NCI/ADR-RES multidrug resistant cell lines at low nanomolar concentrations. Dilep *et al* designed and synthesized a series of benzyl or phenethyl thiazolidinone-indole derivatives and each compound showed excellent antiproliferative activity against A549, NCI-H460, MDA-MB-231, HTC-29 and HCT-15 cancer cells [29]. Compounds might have stronger antiproliferative activity when they contained a phenethyl thiazolidinone structure but the antiproliferative activity was decreased when the hydrogen atom of the indole nitrogen was replaced by an aliphatic chain. Among which, the optimal compound **14** (Fig. 2) showed good cytotoxic effect on HCT-15 and HCT-29 cells. Since compound ABI-231 (Fig. 2) exerted its antiproliferative effect by interacting with colchicine binding site, it is currently being evaluated as an oral formulation in clinical trials for prostate cancer. Wang's research group has been investigating ABI-231 derivatives by modifying the structure of the lead compound [30]. Among them, the antiproliferative activity of the optimal compound **15** (Fig. 2) was stronger than that of ABI-231. The IC_{50} value against WM164 cells was 1.6 nM and in A375 and M14 cells was from 3.6 nM to 3.7 nM. The SAR analysis suggested that the indole benzene ring without substituent was the most potent structure. When indole was linked with an imidazole group attached at positions 5 and 6, its antiproliferative activity on A375 cells was equivalent to that of lead compound ABI-231. The compound **15**, obtained when the imidazole was attached to the 4-position of indole, showed an approximately two-fold increase in antiproliferative activity on A375 cell lines (IC_{50} = 3.6 nM) and almost five-fold increase on WM164 cell lines (IC_{50} = 1.6 nM) compared to the ABI-231 (IC_{50} = 8.1 nM and 7.2 nM respectively). Further studies showed that compound **15** could significantly inhibit the taxol-resistant PC-3 cell lines with IC_{50} value of 66.9 nM. According to research from Cui *et al*, a series of novel indazole derivatives were designed and synthesized as tubulin inhibitors [31]. SAR studies show that the substitution of a methyl group in the indazobenzene ring can enhance the cytotoxicity whilst the 6-substituted methyl group was better than other positions. The 3,4,5-trimethoxyphenyl fraction at the other side was the preferred choice for obtaining better antiproliferative activity. The GI_{50} of indazole derivatives **16** and **17** (Fig. 2) against HCT116, HepG2 and A549 tumor cells were 15 nM, 27 nM, 33 nM, (compound **16**) and 41 nM, 53 nM, 65 nM (compound **17**) respectively. Compound **16** showed excellent antiproliferative activity on SW620 and HT29 cells, GI_{50} = 8 nM and 31 nM. In the mechanism study, these compounds have been proven to target colchicine, inhibit tubulin polymerization, destroy the cell microtubule network, block cancer cell growth in G2/M phase and induce apoptosis. Romeo *et al* synthesized a new type of tubulin polymerization inhibitor with trimethoxyaniline indole skeleton [32]. The SAR illustrated that trimethoxy substitution on the benzene ring was

beneficial in facilitating cytotoxicity, methoxy substitution of indole 5 or 6 position played an important role in inhibiting cell growth, and indole 2 ester formation could also improve the antiproliferation ability of the compound. The most promising compounds in this series were compound **18** and **19** (Fig. 2), both of which targeted tubulin at colchicine site. Compound **19** was the optimal compound in inhibiting microtubule aggregation with IC_{50} value of 0.37 μM. Multitudes of 1,2,4-triazole-indole-3-methanone derivatives were designed and synthesized by Naaz *et al* [33]. The best of them, compound **20** and compound **21** (Fig. 2), were evaluated for *in vitro* antiproliferative activity and showed IC_{50} values of 2.42 μM and 3.06 μM against MCF-7 cells, respectively, which were more active than adriamycin (IC_{50} = 6.31 μM). The SAR analysis showed that the antiproliferative activity of 2-position substituted electron-withdrawing group on the benzene ring was better than that of the other positions, the fluorine atom was superior to the other electron-absorbing groups and replacing the benzene ring with other aliphatic groups would lead to a significant decrease in activity. Li *et al* discovered a series of new pyrazole[1,5-a]pyrimidine derivatives [34]. Among them, compound **22** (Fig. 2), a pyrazole linked to a 5-position indole group, showed strong antiproliferative activity against a variety of tumor cells (Hela, A549, MCF-7, B16-F10 and HCT-116) with IC_{50} values ranging from 3~48 nM, which notably significantly inhibited the growth of MCF-7 cells with an IC_{50} value of only 3 nM. The SAR analysis showed that the best antiproliferative activity was achieved when the pyrazolopyrimidine ring was attached to the 5-position of indole, and the antiproliferative activity was reduced when the N-1 hydrogen atom of the indole ring was replaced by a methoxy group. When the 3,4,5-methoxybenzene ring was substituted by other rings, its antiproliferative activity decreased. Further studies showed that compound **22** inhibited tubulin aggregation, blocked MCF-7 cells in G2/M phase and inhibited MCF-7 cell migration *in vitro*.

Wu *et al* designed and synthesized a series of indole-based[1,2,4]triazolo[4,3-*a*] pyridine derivatives as novel inhibitors of microtubule aggregation [35]. *In vitro* bioassays showed that compound **23** (Fig. 2) exhibited strong antiproliferative activity against HeLa, A549, MCF-7 and HCT116 cells with IC_{50} values of 15, 69, 49 and 33 nM respectively. Pecnard *et al* have synthesized derivatives containing pyridine-linked indoles [36]. By SAR analysis, pyridine was superior to the benzene ring when used as a linkage group between indole and quinoline, whilst substitution of the H-atom at the *N*-1 position of indole or the presence of an electron-withdrawing substituent on the benzene ring reduced the antiproliferative activity of the compounds. *In vitro* antiproliferative bioassay, compound **24** (Fig. 2) showed excellent antiproliferative activity against HCT116 cells with IC_{50} = 2.2 nM, which was equivalent to the activity of positive control combretastatin A-4 (CA-4) (IC_{50} = 2.6 nM). Compound **24** showed the best antiproliferative activity (IC_{50} = 2.0 nM) on K562R cells with MDR1 overexpression, which was several times higher than that of positive drug. Wang *et al* synthesized a novel series of 2-phenyltetrahydroindole derivatives as inhibitors of tubulin polymerization with the aromatic ring of the indole replaced by an aliphatic ring and hydrazine as the linking chain [37]. The SAR analysis showed that the trimethoxy substitution on the benzene ring was more active than the monosubstituted halogen, and compound **25** (Fig. 2) with

a methoxy substituent at the para position of the benzene ring displayed the strongest antiproliferative activity against MCF-7 and A549 cells with IC_{50} values of 1.77 μM and 3.75 μM respectively, more than three times higher than the CA-4 positive control. In the work reported in 2021, Rungroj *et al* identified several 3-phenyl-1H-indole derivatives with antiproliferative activity by screening commercial databases of compounds [38]. These molecules were evaluated for inhibition of microtubule aggregation, and SAR revealed that the change of the oxygen atom in the furan ring to a sulphur atom significantly improved the antiproliferative activity (Fig. 2). Compound **26** had the optimal activity on MOLT-3 cells with IC_{50} value of 70 nM, while the introduction of an electron-donating group at the furan oxygen atom can further optimize the cytotoxicity against HuCCA-1 tumor cells, and compound **27** with methoxy substitution displayed the best activity against HuCCA-1 and MOLT-3 cells with IC_{50} values of 60 nM and 90 nM respectively. The compounds with chalcone linkage designed by Hawash group also have the potent antiproliferative activity against cancer cell lines [39]. Bongkotrat *et al* designed and synthesized a series of 2,3-diarylindole derivatives as inhibitors of microtubule polymerization [40]. *In vitro* bioassays showed that compound **28** (Fig. 2) exhibited moderate antiproliferative activity against A549 cell line with IC_{50} value of 5.17 μM. Wang *et al* designed and synthesized new indoline derivatives and investigated their antiproliferative activity *in vitro* [41]. The IC_{50} values of the optimal compound **29** (Fig. 2) against MGC-803, A549 and Kyse30 cell lines were 1.84 μM, 6.82 μM and 1.61 μM, respectively. Diao *et al* designed and synthesized a series of novel indole-based oxalamide and aminoacetamide derivatives [42]. The IC_{50} values of the optimal compound **30** (Fig. 2) for HeLa, HCT116 and PC-3 cells were ranging from 11.99 μM to 15.41 μM. Flow cytometric analysis demonstrated the compound **30** induced the cell cycle arrest at G2/M phase in HeLa cell lines. Valery *et al* designed and synthesized a series of Indibulin (D-24851) derivatives with bisphosphonate fragment as inhibitors of microtubule polymerization [43]. Among them, compound **31** (Fig. 2) showed the best anti-tumor activity with IC_{50} values of 0.034 μM, 0.223 μM, 0.222 μM, 0.478 μM and 0.658 μM against A375, A549, HST116, DU145 and T47D cell lines, respectively. Chen *et al* synthesized a series of 3-amidoindole derivatives possessing 3,4,5-trimethoxylphenyl groups as colchicine polymerization inhibitors [44]. The IC_{50} values of the optimal compound **32** (Fig. 2) against MDA-MB-231, BT549 and T47D cells were ranging from 0.04 ~ 6.43 μM. Mechanism study demonstrated that compound **32** significantly inhibited growth of breast cancer cells through arresting cell cycle in G2/M phase via a concentration-dependent manner.

2.2. Trimethoxyphenyl or its analogue moiety as the crucial pharmacophore

In addition to the indole ring structure, 3,4,5-trimethoxyphenyl plays a crucial role in the structural domain of CBSIs. Most derivatives containing 3,4,5-trimethoxyphenyl significantly enhanced the antiproliferative activity *in vitro*. For example, Zhai *et al* designed a series of phenyl pyrazolo[3,4-b]pyridine microtubule polymerization inhibitors targeting the colchicine binding site and evaluated the antiproliferative activity [45]. Most compounds showed excellent

antiproliferative activity against SGC-7901 and HeLa cells but were less sensitive to A549 cells. However, the most potent compound **33** (Fig. 3) significantly inhibited microtubule protein aggregation. SAR analysis showed that the cytotoxicity against A549 cells was significantly enhanced by the substitution of methyl groups in the para position of benzene ring, while other substituents such as halogen and methoxy groups were not effective, and the trimethoxyphenyl was essential for the activity of this compound. Yin *et al* designed and synthesized a series of novel resveratrol cinnamoyl hybrids as tubulin polymerization inhibitors [46] and tested the antiproliferative activity of five cancer cell lines such as A549, MCF-7, HepG2, HeLa and MDA-MB231. Most of these compounds showed good antiproliferative activity. In particular, trimethoxyphenyl substituted on the terminal benzene ring had the best cytotoxicity, whilst other methyl or methoxy single substitutions of the benzene ring did not significantly improve the effect. The halogen substituent has certain antiproliferative activity, but the substitution of strong electron-withdrawing groups leads to the loss of activity. The IC_{50} values of the optimal compound **34** (Fig. 3) against A549 cell lines (IC_{50} = 0.12 μM) were much better than the control colchicine (IC_{50} = 1.17 μM). Jiang *et al* discovered novel and effective trimethoxyphenyl azole derivatives as tubulin inhibitors [47], in which amino substituted compound **35** (Fig. 3) showed IC_{50} values of 1 nM for both human colon cancer cell lines COLO205 and HCT-116 cells with IC_{50} values of 1.6 μM for inhibiting microtubule polymerization. Compound **36** substituted by fluorine atoms performed equally well, with IC_{50} value of 2 nM for COLO205 cells. The substitution by aliphatic group on the N-1 of oxazole lead to a significant reduction in antiproliferative activity. Chen *et al* designed and synthesized a series of 3,4,5-trimethoxyphenylpyridine compounds [48] by optimizing the structure of lead compound ABI-231. Through SAR analysis, the indole ring of ABI-231 was replaced by benzene ring and the B ring was replaced by pyridine ring from imidazole to increase the antiproliferative activity of the compounds. Compound **37** (Fig. 3) with 3-hydroxy-4-methyl functional group introduced into the benzene ring showed effective antiproliferative activity against breast cancer cell line MDA-MB-231, MDA-MB-453 and SK-BR-3 with IC_{50} values of 1.7 nM, 1.2 nM, 2.8 nM respectively, and for melanoma cell lines A375, M14 and RPMI7951 with IC_{50} values of 1.5 nM, 1.7 nM and 2.7 nM. Compound **37** can induce tubulin depolymerization and enact a significant antiproliferative effect that led to the apoptosis of tumor cells in a dose-dependent manner. The IC_{50} of paclitaxel resistant cells was significantly better than that of colchicine and paclitaxel control.

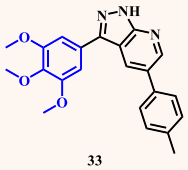

33

Cell growth inhibition
IC_{50} = 13 nM (SGC-7901)
IC_{50} = 82 nM (A549)
IC_{50} = 45 nM (HeLa)
Tubulin polymerization inhibition
IC_{50} = 37.5 μM

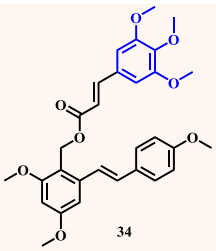

34

Cell growth inhibition
IC_{50} = 0.37 μM (Hela)
IC_{50} = 0.12 μM (A549)
IC_{50} = 0.44 μM (HepG2)
IC_{50} = 0.016 μM (MCF-7)
IC_{50} = 0.78 μM (MDA-MB-231)
Tubulin polymerization inhibition
IC_{50} = 1.03 μM

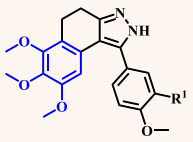

35: $R^1 = NH_2$
36: $R^1 = F$

Cell growth inhibition
35: IC_{50} = 1 nM (COLO205)
IC_{50} = 1 nM (HCT-116)
36: IC_{50} = 2 nM (COLO205)
Tubulin polymerization inhibition
35: IC_{50} = 1.6 μM
36: IC_{50} = 9.2 μM

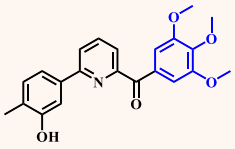

37

Cell growth inhibition
IC_{50} = 1.7 nM (MDA-MB-231)
IC_{50} = 1.2 nM (MDA-MB-453)
IC_{50} = 2.8 nM (SKBR3)
IC_{50} = 1.5 nM (A375)
IC_{50} = 1.7 nM (M14)
IC_{50} = 2.7 nM (RPMI7951)

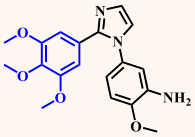

38

Cell growth inhibition
IC_{50} = 0.09 μM (MDA-MB-468)
IC_{50} = 1.04 μM (MDA-MB-231)
IC_{50} = 0.5 μM (T47D)
IC_{50} = 0.1 μM (HCT15)
IC_{50} = 0.2 μM (HT-29)
IC_{50} = 0.08 μM (HeLa)
Tubulin polymerization inhibition
IC_{50} = 0.4 μM

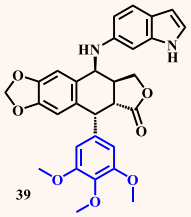

39

Cell growth inhibition
IC_{50} = 0.08 μM (Hela)
IC_{50} = 0.08 μM (A549)
IC_{50} = 0.1 μM (HepG2)
IC_{50} = 0.07 μM (MCF-7)

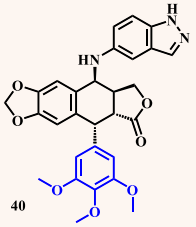

40

Cell growth inhibition
IC_{50} = 0.2 μM (Hela)
IC_{50} = 0.2 μM (A549)
IC_{50} = 0.3 μM (HepG2)
IC_{50} = 0.2 μM (MCF-7)

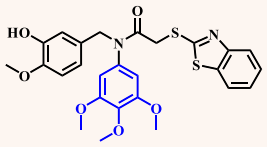

41

Cell growth inhibition
IC_{50} = 0.035 μM (MGC-803)
IC_{50} = 0.182 μM (HCT-116)
IC_{50} = 2.11 μM (PC-3)
IC_{50} = 0.2 μM (MCF-7)
IC_{50} = 0.049 μM (SGC-7901)
Tubulin polymerization inhibition
IC_{50} = 1.9 μM

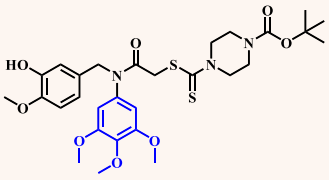

42

Cell growth inhibition
IC_{50} = 0.082 μM (MGC-803)
IC_{50} = 0.128 μM (HCT-116)
IC_{50} = 0.069 μM (Kyse30)
IC_{50} = 0.078 μM (Kyse450)

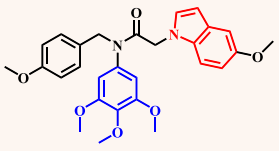

43

Cell growth inhibition
IC_{50} = 1.56 μM (MGC-803)
IC_{50} = 3.56 μM (PC-3)
IC_{50} = 14.5 μM (EC-109)

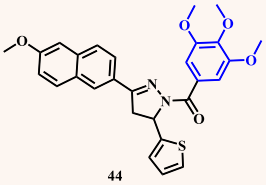

44

Cell growth inhibition
IC_{50} = 2.50 μM (HepG2)
IC_{50} = 2.46 μM (HeLa)
IC_{50} = 1.19 μM (MCF-7)
Tubulin polymerization inhibition
IC_{50} = 1.47 μM

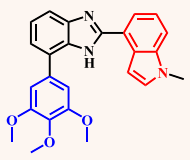

45

Cell growth inhibition
IC_{50} = 85 nM (A549)
IC_{50} = 68 nM (HeLa)
IC_{50} = 18 nM (MCF-7)
IC_{50} = 29 nM (B16-F10)
Tubulin polymerization inhibition
IC_{50} = 2.52 μM

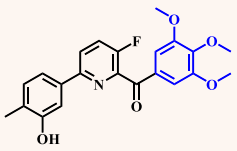

46

Cell growth inhibition
IC_{50} = 2.2 nM (MDA-MB-231)
IC_{50} = 1.4 nM (MDA-MB-453)
IC_{50} = 4.8 nM (SKBR3)
IC_{50} = 1.8 nM (A375)
IC_{50} = 1.9 nM (M14)
IC_{50} = 2.4 nM (RPMI7951)

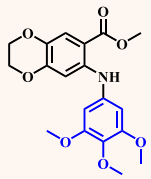

47

Cell growth inhibition
IC_{50} = 0.24 μM (A549)
IC_{50} = 0.10 μM (MDA-MB-231)
IC_{50} = 0.035 μM (HeLa)
IC_{50} = 0.14 μM (MCF-7)
IC_{50} = 0.023 μM (HT29)
Tubulin polymerization inhibition
IC_{50} = 1.09 μM

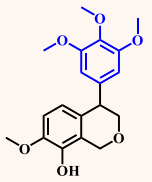

48

Cell growth inhibition
IC_{50} = 22 nM (MDA-MB-231)
IC_{50} = 25 nM (KB)
IC_{50} = 10 nM (K562)
IC_{50} = 11 nM (H22)
IC_{50} = 95 nM (LO2)

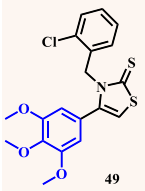

49

Cell growth inhibition
IC_{50} = 5.62 μg/mL (A549)
IC_{50} = 1.14 μg/mL (MCF-7)
IC_{50} = 5.50 μg/mL (SKOV3)

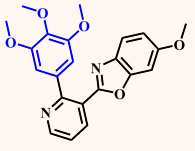

50

Cell growth inhibition
GI_{50} = 2.1 μM (HT-29)
GI_{50} = 0.89 μM (A549)
GI_{50} = 0.27 μM (U251)
Tubulin polymerization inhibition
IC_{50} = 2.1 μM

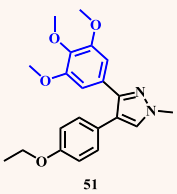

51

Cell growth inhibition
IC_{50} = 16.7 nM (SKOV3)
IC_{50} = 31.4 nM (MDA-MB-231)
IC_{50} = 32.8 nM (HeLa)
IC_{50} = 67.0 nM (A549)
IC_{50} = 58.0 nM (CT26)
IC_{50} = 35.4 nM (MCF-7)

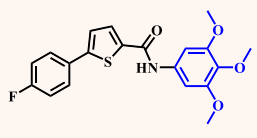

52

Cell growth inhibition
IC_{50} = 5.46 μM (Hep3B)
IC_{50} = 29.74 μM (MCF-7)
IC_{50} = 35.08 μM (Colo205)

Fig. 3 Chemical structures of compounds **33~52**

Li *et al* designed and synthesized a series of novel trimethoxyphenylimidazole derivatives based on the structure of 2-aryl-4-benzoylimidazole analogues and CA-4 [49]. Among them, compound **38** (Fig. 3) showed the best anti-tumor activity with IC_{50} values of 0.09 μM, 1.04 μM, 0.50 μM, 0.10 μM, 0.20 μM and 0.08 μM against MDA-MB-468, MDA-MB231, T47D, HCT15, HT-29 and Hela cells, respectively. *In vivo* pharmacodynamic study suggested that compound **38** had a highly effective inhibitory effect on tumor growth in MDA-MB-468 nude mice xenotransplantation model. Zhao *et al* performed their research from the podophyllotoxin on the structural domains of previously crystallised proteins and found that the potential binding site of aT5-loop-aH7 near the colchicine structural domain facilitated the introduction of a high affinity benzoheterocycle to modify the structure of the onychotoxin [50] for improving tubulin binding affinity. Compound **39** and compound **40** (Fig. 3) exhibited good antitumor effects against HepG-2, HeLa, A549 and MCF-7 cells. Song *et al* designed and synthesized new benzothiazole tertiary amide derivatives and investigated their antiproliferative activity *in vitro* against three kinds of cancer cells (MGC-803, HCT-116 and PC-3 cells) [51]. Through SAR analysis, it was found that 3,4,5-trimethoxyphenyl was one of the key structures and the 3-position substituted amino or hydroxyl of the benzene ring could significantly improve the antiproliferative activity, and hydroxyl substitution was better. The activity for benzothiazole ring was the best, and any substituent group on the benzene ring will significantly weaken the antiproliferative activity. The optimal compound **41** (Fig. 3) showed excellent antiproliferative activity against MGC-803, HCT-116, PC-3, MCF-7 and SGC-7901 cells. The binding of compound **41** to the colchicine binding site of tubulin effectively inhibited microtubule polymerisation with an IC_{50} = 1.9 μM. Sun *et al*. designed novel bis-substituted aromatic amide dithiocarbamate derivatives based on the structure designed in previous studies, replacing the thioether benzothiazole with a dithiocarbamate [52]. The 3,4,5-trimethoxyphenyl group remained and played an important role, with the benzene ring 3-hydroxy-4-methoxy substitution significantly increasing the antiproliferative activity. The results of the bioactivity evaluation showed that compound **42** (Fig. 3) exhibited the strongest antiproliferative activity against a variety of tumor cells (MGC-803, HCT-116, Kyse30 and Kyse450). Molecular docking results showed that compound **42** could bind to the colchicine binding site of tubulin through hydrogen bonds with residues Leu246 and Tyr200, and hydrophobic interactions with residues Thr179, Val181, Tyr200, Val236, Thr237, Leu240 and Ala314. Liu *et al* designed and synthesized a series of diarylamide nitrogen-containing heterocyclic derivatives [53] containing 3,4,5-trimethoxyphenyl with some structural similarity to the compound by Song's research group (Fig. 3) but with a 5-methoxyindole group attached to the key structure (compound **43**), which also showed moderate antiproliferative activity. Yang *et al* revealed kinds of pyrazoline derivatives with characteristic 3,4,5-trimethoxyphenyl and thiophene moieties as tubulin polymerization inhibitors [54]. The ability of 3,4,5-trimethoxyphenyl to interact with multiple amino acid residues in the colchicine pocket site was the crucial point to the antiproliferative

activity of the derivatives. The naphthalene aromatic ring of the optimal compound **44** (Fig. 3) could form hydrophobic interactions with multiple amino acid residues and exhibited good antiproliferative activity in cancer cell lines. Ren *et al* designed and synthesized novel indazole benzimidazole derivatives as tubulin inhibitors [55]. Taking 3,4,5-trimethoxyphenyl and imidazole as the pivotal pharmacophore, it has a strong antiproliferative effect. Among them, compound **45** (Fig. 3) showed the strongest antiproliferative effect on MCF-7, A549, HeLa and B16-F10 cells with the IC_{50} values ranged from 18 nM to 85 nM. Compound **45** effectively overcame paclitaxel resistance *in vitro*. The IC_{50} values of paclitaxel resistant cell lines A2780/T and A2780S were 9.7 nM and 6.2 nM respectively, and the resistance index (RI) was only 1.6 better than colchicine (46.9). Chen *et al* designed and synthesized a series of biphenyltrimethoxyphenyl ketone derivatives [56], in which compound **46** (Fig. 3) showed potent antiproliferative activity. The IC_{50} values against MDA-MB-231, MDA-MB-453, SKBR3, A375, M14 and RPMI7951 cells with an average of 2.4 nM. Moreover, compound **46** also had strong antiproliferative activity to paclitaxel resistant cell lines compared with colchicine and paclitaxel. The resistance index (RI) was only 1.8. A series of diphenylamine derivatives [57] were designed and synthesized by Yan *et al*. Compound **47** (Fig. 3), containing a dioxohexa ring, inhibited tubulin polymerization with an IC_{50} value of only 0.035 μM in HeLa cells, and arrested the HT29 cell cycle in G2/M phase with an IC_{50} value of 0.023 μM. The drug-resistance index for MCF-7/TxR resistant strain was 1.3, which was lower than that of positive control CA-4 (1.8). Our group extracted a natural compound (±)-7,8-dihydroxy-3-methylisochroman-4-one from the peel of a plant *Musa sapien tum L* and the structure was modified to obtain a series of 4-aryisochromene derivatives as tubulin polymerization inhibitors [58]. The optimal compound **48** (Fig. 3) had strong antiproliferative activity against KB, HCT-8, MDA-MB-231, K562, H22, and LO2 cancer cell lines with IC_{50} values ranging from 10 nM to 95 nM. Further mechanistic studies showed that compound **48** destroyed the intracellular microtubule network, led to G2/M phase arrest, induced apoptosis, and depolarized the mitochondria of K562 cells. Mahsa *et al* designed a series of thiazole-2(3*H*)-thiones derivatives containing 4-(3,4,5-trimethoxyphenyl) moiety [59]. The results indicated that the optimal compound **49** (Fig. 3) exhibited significant antiproliferative activity against A549, MCF-7 and SKOV3 cells with IC_{50} values of 5.62 μg/mL, 1.14 μg/mL and 5.50 μg/mL respectively. He *et al* designed and synthesized a series of novel benzo[*d*]imidazole, benzo[*d*]thiazole, and benzo[*d*]oxazole derivatives as tubulin inhibitors [60]. Among them, the optimal compound **50** (Fig. 3) showed potent antiproliferative activity against HT-29, A549 and U251 cancer cell lines with IC_{50} values ranging from 0.27 ~ 2.1 μM. Further investigations showed that compound **50** displayed strong tubulin polymerization inhibitory activity (IC_{50} = 2.1 μM). Lai *et al* synthesized a series of *cis*-restricted pyrazole analogues of combretastatin A-4 as inhibitors of tubulin polymerization [61]. The representative compound **51** (Fig. 3) showed significant antiproliferative activity against SKOV3, MDA-MB-231, HeLa, A549, CT26 and MCF-7 cells *in vitro*, with IC_{50} values ranging from 16.7 ~ 67 nM. Hawash's group designed and synthesized a series of novel trimethoxyphenyl scaffold derivatives as tubulin polymerization inhibitors targeting at colchicine

binding site [62], and the optimal compound **52** (Fig. 3) showed potent antiproliferative activity against Hep3B, MCF-7 and Colo205 cancer cell lines with IC_{50} values of 5.46 μM, 29.74 μM and 35.08 μM, respectively.

2.3. Properties and effect of using triazole ring or its analogues as a linker

Researchers have discovered that the triazole ring, as a linker between different structural domains, can be a good replacement for the original structure and allows the compounds to exert better antiproliferative activity. Triazoles have become an important option in the compound modification strategy. Xu' s group has designed and synthesized a series of novel 3,6-diaryl-7*H*-[1,2,4]triazolo[3,4-b][1,3,4]thiadiazine derivatives [63]. Among these compounds, compound **53** (Fig. 4) showed high degree of binding to tubulin at the colchicine binding site, thus exerting the strongest antiproliferative activity against three human tumor cell lines, SGC-7901, A549 and HT-1080 with IC_{50} values between 11-15 nM, close to the positive control CA-4. After SAR studies, the 3,4,5-trimethoxyphenyl group, which played a key antiproliferative role in CA-4, could be replaced with 3-methoxyphenyl and 4-methoxyphenyl, among others, and maintained significant antiproliferative activity. Fu *et al* designed and synthesized trimethoxyphenyltriazole derivatives [64]. The optimal compound **54** containing coumarin fragment and trimethoxyphenyl-1,2,3-triazole (Fig. 4) exhibited the best antiproliferative activity with IC_{50} values of 0.34 μM, 0.13 μM and 1.74 μM for PC3, MGC803 and HepG2 cells, respectively. Through the SAR analysis, coumarin fragments and 3,4,5-trimethoxyphenyl were determined to be essential for antiproliferative activity and the substitution of the coumarin fragment into other aromatic groups resulted in a significant decrease in activity. Qi *et al* synthesized a series of 1-(benzofuran-3-yl)-4-(3,4,5-trimethoxyphenyl)-1*H*-1,2,3-triazole derivatives [65]. Taking triazole as the linking chain, 3,4,5-trimethoxyphenyl played an important role in antitumor activity while compound **55** with benzofuran-2-formamide linking triazole (Fig. 4) revealed the most potent antiproliferative activity, with IC_{50} values of 0.87 μM, 0.73 μM and 0.57 μM for HCT-116, HeLa and A549 cells, respectively. Compound **55** effectively inhibited tubulin polymerization, caused cell stagnation in G2/M phase, and subsequently led to apoptosis.

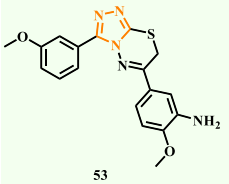

53

Cell growth inhibition
IC_{50} = 11 nM (SGC-7901)
IC_{50} = 15 nM (A549)
IC_{50} = 14 nM (HT-1080)
Tubulin polymerization inhibition
IC_{50} = 1.6 μM

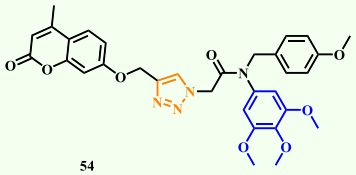

54

Cell growth inhibition
IC_{50} = 0.34 μM (PC3)
IC_{50} = 0.13 μM (MGC803)
IC_{50} = 1.74 μM (HepG2)
Tubulin polymerization inhibition
IC_{50} = 2.164 μM

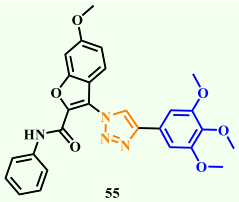

55

Cell growth inhibition
IC_{50} = 0.87 μM (HCT-116)
IC_{50} = 0.73 μM (HeLa)
IC_{50} = 5.74 μM (HepG2)
IC_{50} = 0.57 μM (A549)
Tubulin polymerization inhibition
IC_{50} = 4.1 μM

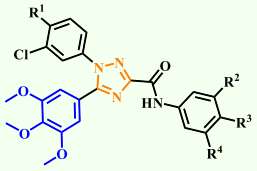

56: R^1 = F, R^4 = OF_3, R^2, R^3, = H
57: R^1 = OCH_3, R^2, R^3, R^4 = F
58: R^1 = F, R^2 = OCH_3, R^3, R^4 = H
59: R^1 = OCH_3, R^4 = OCF_3, R^2, R^3, = H

Cell growth inhibition IC_{50}

	HepG2	HL-60	MCF-7
56	0.10 μM	0.16 μM	0.31 μM
57	0.04 μM	2.66 μM	2.10 μM
58	0.35 μM	0.004 μM	0.02 μM
59	7.11 μM	0.81 μM	0.039 μM

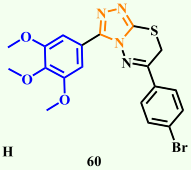

60

Cell growth inhibition
IC_{50} = 12 nM (HeLa)
IC_{50} = 40.40 μM (MCF-7)
IC_{50} = 10.40 μM (A549)
IC_{50} = 27.91 μM (T47D)
Tubulin polymerization inhibition
IC_{50} = 3.4 μM

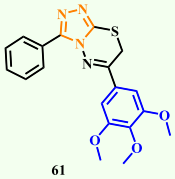

61

Cell growth inhibition
IC_{50} = 0.70 μM (MCF-7)
IC_{50} = 4.63 μM (SKOV3)
IC_{50} = 3.71 μM (A549)
Tubulin polymerization inhibition
IC_{50} = 1.61 μM

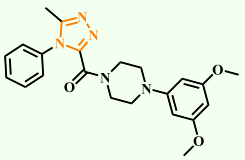

62

Cell growth inhibition
IC_{50} = 0.403 μM (HeLa)
IC_{50} = 2.16 μM (SGC-7901)
IC_{50} = 2.21 μM (A549)

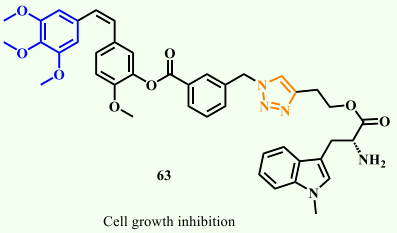

63

Cell growth inhibition
IC_{50} = 0.07 μM (HeLa)
IC_{50} = 0.46 μM (PC-3)
IC_{50} = 0.22 μM (A549)

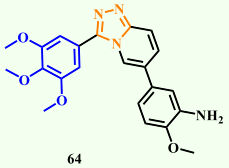

64

Cell growth inhibition
IC_{50} = 12 nM (HeLa)
IC_{50} = 40.40 μM (MCF-7)
IC_{50} = 10.40 μM (A549)
IC_{50} = 27.91 μM (T47D)
Tubulin polymerization inhibition
IC_{50} = 3.4 μM

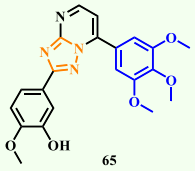

65

Cell growth inhibition
IC_{50} = 0.06 μM (HeLa)
IC_{50} = 0.24 μM (HT29)
IC_{50} = 6.05 μM (A549)
IC_{50} = 3.49 μM (T47D)
IC_{50} = 14.69 μM (HepG2)
IC_{50} = 18.43 μM (HCT-116)
Tubulin polymerization inhibition
IC_{50} = 1.3 μM

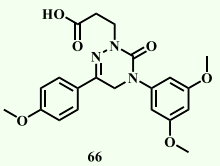

66

Cell growth inhibition
IC_{50} = 10.9 μM (MCF-7)
IC_{50} = 8.2 μM (HepG2)
IC_{50} = 15.7 μM (HCT-116)
Tubulin polymerization inhibition
IC_{50} = 3.9 μM

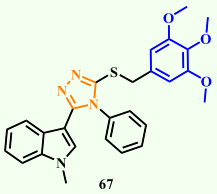

67

Cell growth inhibition
IC_{50} = 0.38 μM (MCF-7)
IC_{50} = 0.23 μM (HepG2)
IC_{50} = 0.30 μM (A549)
IC_{50} = 0.15 μM (HeLa)
Tubulin polymerization inhibition
IC_{50} = 2.10 μM

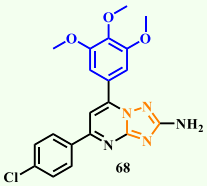

68

Cell growth inhibition
IC_{50} = 0.53 μM (HCT-116)
Tubulin polymerization inhibition
IC_{50} = 3.84 μM

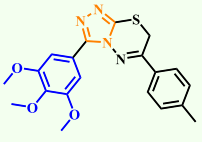

69

Cell growth inhibition
IC_{50} = 4 nM (HeLa)
IC_{50} = 50 nM (A549)
IC_{50} = 98 nM (MCF-7)
Tubulin polymerization inhibition
IC_{50} = 1.69 μM

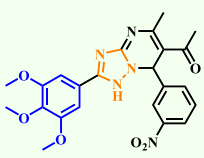

70

Cell growth inhibition
IC_{50} = 0.75 μM (HeLa)
IC_{50} = 1.02 μM (A549)

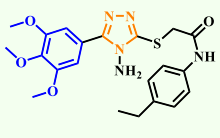

71

Cell growth inhibition
IC_{50} = 0.05 μM (HeLa)
IC_{50} = 0.84 μM (HT-29)

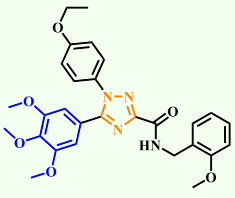

72

Cell growth inhibition
IC_{50} = 0.62 μM (HepG2)
IC_{50} =0.60 μM (HL-60)

Fig. 4 Chemical structures of compounds **53~72**

Mustafa *et al* designed a series of 1,2,4-triazole derivatives based on the structural modification of CA-4 [66]. The results indicated that compounds **56** and **57** (Fig. 4) showed significant tubulin inhibition on HepG2 cells compared to CA-4, with IC_{50} values of 100 nM and 40 nM, respectively, while on HL-60 cells, the IC_{50} values for compounds **58** and **56** were 4 nM and 16 nM, respectively. The IC_{50} value of compound **59** (Fig. 4) against MCF-7 was 39 nM. Molecular docking showed that the tubulin binding affinity of compound **58** was almost equal to that of CA-4. Ansari *et al* identified a series of trimethoxyphenyl 4*H*-1,2,4-triazole compounds. The outcome of molecular docking showed that the compounds interacted on colchicine binding sites and exerted the effect of tubulin inhibition, and the IC_{50} value of compound **60** (Fig. 4) on SKOV3 cells was 0.30 μM [67]. Exchanging the position of 3,4,5-trimethoxyphenyl and benzene ring could exert significant toxic effects on different tumor cells. For example, the IC_{50} value of rigid analogue compound **61** on MCF-7 cells was 0.7 μM. When 4-bromo group in compound **60** was replaced by 4-methyl, the antiproliferative activity of A549 cells would noticeably increase (IC_{50} = 0.6 μM）. Wang *et al* designed and synthesized a series of novel 5-methyl-4-aryl-3-(4-arylpiperazine-1-carbonyl)-4*H*-1,2,4-triazoles as tubulin inhibitors [68]. Among them, the benzene ring 3,5-disubstituted methoxy compound **62** (Fig. 4) showed moderate activity against three cancer cell lines, SGC-7901, A549 and HeLa (IC_{50} = 2.16 μM, 2.21 μM and 0.403 μM, respectively). Hua *et al* designed and revealed kinds of novel triazole ring-coupled compounds of indoleamine-2,3-dioxygenase and classical tubulin inhibitors [69]. The optimal compound **63** (Fig. 4), consisting of two parts, CA-4 and D-MT, linked by a triazole ring (Fig. 4), showed the most potent anti-tumor activity against the HeLa cancer cell line with an IC_{50} value of 70 nM, which was superior to CA-4 (IC_{50} = 0.21 μM) and with an IC_{50} value of 0.22 μM against A549 cells, which was twice as high as the positive control sample CA-4. The D-MT portion of the coupling could exert synergistic antitumor effects by inhibiting IDO expression. Yang *et al* discovered novel [1,2,4]triazolyl[4,3-a]pyridine with 3,4,5- trimethoxyphenyl as a tubulin polymerization inhibitor [70]. Based on the CA-4 structure, the IC_{50} value of compound **64** (Fig. 4) with benzotriazole ring as the linker and maintaining similar configuration against HeLa was only 12 nM, almost equivalent to that of the positive control CA-4. Molecular docking analysis showed that compound **64** bound to the colchicine potency pocket of tubulin and interacted with surrounding amino acid residues. Huo *et al* came up with a series of novel 2,7-diaryl-[1,2,4]triazolo[1,5-a]pyrimidine derivatives as tubulin polymerization inhibitors based on the classical 3,4,5-trimethoxyphenyl structure of CA-4 [71], with benzotriazole ring as connecting chain, 3-hydroxy-4-methoxy substituted benzene compound **65** (Fig. 4) showed excellent antiproliferative activity to HeLa cells with the IC_{50} value of 60 nM. Compound **65** inhibited tubulin polymerization with IC_{50} value of 1.3 μM, which was three times higher than the positive control CA-4, and the inhibition rate reached to 94%. Eissa *et al* designed and synthesized several new triazole derivatives as tubulin inhibitors [72]. Compound **66** (Fig. 4) effectively

inhibited microtubule assembly, with an IC_{50} value of 3.9 μM, which was better than colchicine and close to the positive control CA-4. SAR analysis showed that the 3,5-dimethoxyphenyl could effectively improve the antiproliferative activity, and the benzene ring of triazole had better activity of para-substituted methoxy. Triazoles as linking chains, carboxylic acids, esters or amides on the nitrogen atom were favourable for increasing the activity. Wu *et al* designed and synthesized a series of indole-1,2,4-triazole derivatives as new tubulin polymerization inhibitors [73]. Through SAR analysis of phenyl substituents, it was found that the interaction between 3,4,5-trimethoxyphenyl structure and surrounding amino acid residues at the colchicine binding site could significantly improve the antiproliferative activity. Compound **67** (Fig. 4) showed significant antiproliferative activity against HepG2, HeLa, MCF-7 and A549 cells *in vitro*, with IC_{50} values ranging from 0.15 μM to 0.38 μM. The capacity of compound **67** to inhibit tubulin polymerization was better than that of positive control colchicine, with IC_{50} value of 2.1 μM. Heba *et al* designed and synthesized a series of 1,2,4-triazolo[1,5-α]pyrimidine derivatives as tubulin polymerization inhibitors at colchicine binding sites through structural modification on the classical compound CA-4 [74]. The triazolopyrimidine ring replaced the double bond in CA-4 as the connecting chain of the two crucial pharmacophores, in which the benzene ring was substituted by 4-chlorine and the trimethoxyphenyl 1,2,4-triazolopyrimidine compound **68** (Fig. 4) showed moderate antiproliferative activity with IC_{50} value of 0.53 μM for HCT-116 cancer cell line. Tubulin polymerization inhibition activity was slightly inferior to the positive control CA-4 with IC_{50} value of 3.84 μM. Ma *et al* designed and synthesized a series of novel triazolothiadiazine derivatives as tubulin inhibitors [75], in which the optimal compound **69** (Fig. 4) showed remarkable antiproliferative activity with IC_{50} values against HeLa, A549 and MCF-7 cell lines of 4 nM, 50 nM and 98 nM respectively. Mechanism study showed compound **69** induced cell apoptosis by up-regulating cleaved PARP and caspase-3 expressions and caused G2/M cell cycle arrest by regulation of p-cdc2 and cyclin B1 expressions. Yang *et al* designed and synthesized a series of novel [1,2,4]triazolo[1,5-a]pyrimidine derivatives as tubulin polymerization inhibitors [76]. The IC_{50} values of optimal compound **70** (Fig. 4) were 0.75 μM and 1.02 μM on HeLa and A549 cell lines respectively. The group of Yang *et al* also designed and synthesized a series of 3,4,5-trimethoxyphenyl substituted triazolylthioacetamides derivatives as potent inhibitors of tubulin polymerization [77]. Among them, compound **71** showed IC_{50} values of 0.05 μM and 0.84 μM against HeLa and HT-29 cells respectively. Muhamad Mustafa *et al* designed and synthesized a series of novel 1,2,4-triazoles derivatives as tubulin inhibitors [78]. The assay *in vitro* revealed that IC_{50} values of optimal compound **72** were 0.62 μM (HepG2) and 0.60 μM (HL-60) respectively. The mechanical analysis showed significant G2/M cell cycle arrest of the compound **72** in HepG2 cells.

2.4. Quinazoline derivatives display potent antiproliferative activity

As reported recently, Li *et al* in our group designed and synthesized a series of novel quinazoline-based microtubule inhibitors and these new compounds showed excellent

antiproliferative activity against human cancer cell lines [79]. The optimal compound **73** (Fig. 5) against K562, HepG2, KB, HCT-8 and MDB-MB-231 were 0.10 μM, 0.11 μM, 0.11 μM, 0.13 μM and 0.12 μM, respectively. The compound **73** occupied three domains of the colchicine binding site and had strong interaction with the surrounding amino acid residues in different domains. The antiproliferative activity of different benzene ring substituents in zone 3 remains, but slightly weaker than compound **73**. For example, the IC_{50} of compounds **74**, **75** and **76** (Fig. 5) to K562 were 0.24 μM, 0.28 μM and 0.31 μM respectively. The growth of the tumor treated with compound **73** at low concentration (15mg/kg) and high concentration (30mg/kg) could be reduced by 50.9% and 62.6% respectively. Liang *et al* has reported a series of tetrahydroquinoline derivatives as tubulin inhibitors with colchicine binding sites [80]. Among them, compound **77** containing 3,4,5-trimethoxyphenyl (Fig. 6) displayed significant antiproliferative activity. Compound **77** inhibited tubulin polymerization and with the increased concentration in HeLa cells.

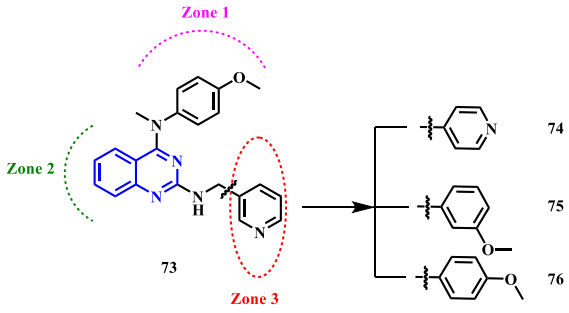

Compd	R	Cell growth inhibition IC_{50}					Tubulin polymerization inhibition
		HepG2	KB	HCT-8	K562	MDA-MB-231	
73		0.11 μM	0.11 μM	0.13 μM	0.10 μM	0.12 μM	2.45 μM
74		0.58 μM	0.48 μM	0.47 μM	0.24 μM	0.46 μM	5.29 μM
75		0.74 μM	1.11 μM	1.17 μM	0.13 μM	1.08 μM	2.67 μM
76	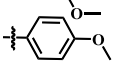	0.21 μM	0.37 μM	0.48 μM	0.28 μM	0.47 μM	5.56 μM

Fig. 5 Chemical structures of compounds **73~76**

According to the report from Ren *et al*., a series of novel acridine and quinoline derivatives were revealed as tubulin inhibitors targeting colchicine binding sites [81]. Compound **78** on B16-F10, HepG-2, HeLa and MCF-7 cells ranged from 0.261 μM to 2.047 μM. Molecular docking outcome exhibited that compound **78** (Fig. 6) was well chimeric with the colchicine binding site of tubulin. If the quinoline ring in compound **78** was replaced by an acridine ring or there were other substituents on the quinoline ring, the antiproliferative activity of the compound would decrease.

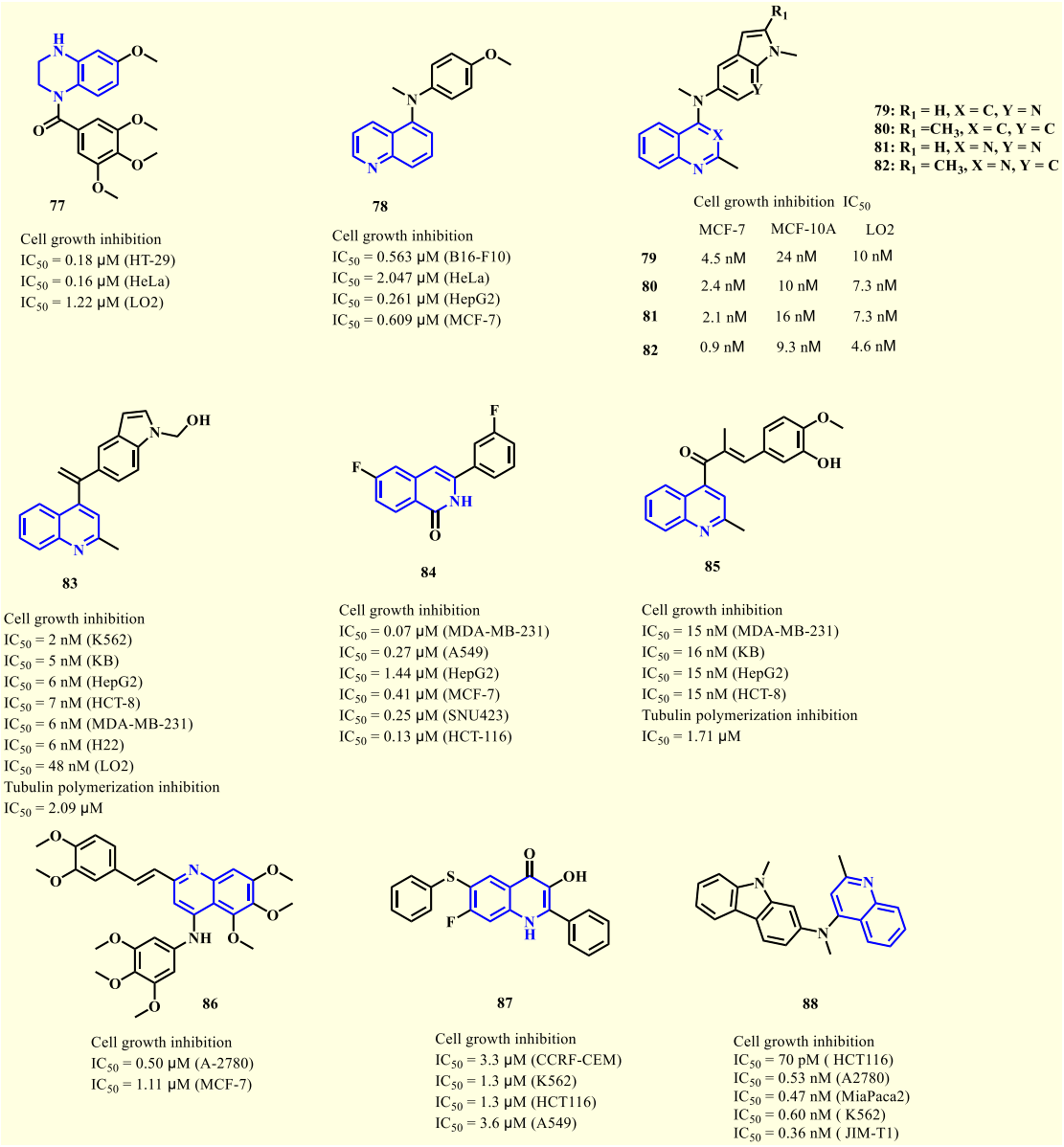

Fig. 6 Chemical structures of compounds **77~88**

Wang *et al* designed and synthesized a series of quinoline-based tubulin inhibitors by combining quinoline rings with indole moieties [82]. After SAR analysis, the replacement of the benzene ring with the indole ring significantly enhanced the antiproliferative activity, for compounds **79** and **80** (Fig. 6) showing IC_{50} values of 4.5 nM and 2.4 nM against MCF-7, respectively. The replacement of the nitrogen atom at position 3 of the quinoline ring further improved the activity, for compound **81** showing an IC_{50} value of 2.1 nM against MCF-7 cells. In addition, compound **82** (Fig. 6) (1 mg/kg) significantly inhibited tumor growth, reducing tumor weight by 81.1%, which was better than the positive control CA-4 (37.5% at 20 mg/kg). As reported in 2019, a series of novel isocombrestatin A-4 (isoCA-4) analogs as effective tubulin polymerization inhibitors were discovered [83]. The optimal compound **83** (Fig. 6) displayed the strongest antiproliferative effect against HepG2, KB, HCT-8, MDA-MB-231, H22 and LO2 cancer cell lines with IC_{50} values

ranging from 6 nM to 48 nM. Through intensive study on SAR, substitution at C-5 position of indole was the most potent, and the hydroxymethyl group was most favored. Reduction of the double bond decreases antiproliferative activity. Elhemely's research group has reported multitudes of quinolone compounds [84]. Only the difference between the 3-position and 4-position of fluorine atom substitution of the benzene ring could lead to a huge discrepancy in antiproliferative activity of up to a hundred times, and the 4-position methoxy substitution would also cause the loss of activity. The IC_{50} values of the 4-fluorine substituted optimal compound **84** (Fig. 6) showed significant cytotoxicity. Molecular docking outcome showed that compound **84** was well aligned with the colchicine binding site of tubulin, resulting in cell cycle arrest in G2/M phase and inducing apoptosis. Li *et al* designed and synthesized a series of novel quinoline-chalcone derivatives [85]. Based on the bioassay results of K562 cells, it can be found that the 3-hydroxy-4-methoxyphenyl moiety can significantly improve the anti-tumor activity and the methyl substituent on the double bond of the leakage chain can stabilize the configuration. The IC_{50} of the optimal compound **85** (Fig. 6) for K562 cells was only 9 nM, and for HepG2, KB, HCT-8 and MDA-MB-231 cells the potent inhibitory effect had IC_{50} values ranging from 15 nM to 16 nM. Salimeh *et al* designed and synthesized a series of novel 5,6,7-trimethoxy-*N*-aryl-2-styrylquinolin-4-amines derivatives as inhibitors of microtubule polymerization [86]. The optimal compound **86** (Fig. 6) showed significant antiproliferative activity against A-2780 and MCF-7 tumor cell lines *in vitro*, with IC_{50} values of 0.50 μM and 1.11 μM respectively. Chen *et al* designed and synthesized a series of novel 2-phenyl-3-hydroxy-4(1*H*)-quinolinone derivatives [87], in which compound **87** (Fig. 6) showed potent antiproliferative activity and the IC_{50} values against CCRF-CEM, K562, HCT116 and A549 cell lines were 3.3 μM, 1.3 μM, 1.3 μM and 3.6 μM respectively. Ilhem *et al* designed and synthesized a series of novel *N*,*N*-bis-heterocyclic-methylamines derivatives as tubulin inhibitors [88]. Among them, the optimal compound **88** (Fig. 6) showed very potent antiproliferative activity against HCT116 cancer cell line with IC_{50} value of 70 pM, and against A2780, MiaPaca2, K562 and JIM-T1 cell lines with IC_{50} values ranging from 0.36 ~ 0.60 nM. Mechanistic studies showed that compound **88** arrested the cellular cycle in G2/M phase of the cellular cycle and induced apoptosis of HCT116 cells.

2.5. Other representative structures with potent tubulin polymerization inhibitory effect

Bueno *et al* reported new cyclohexanedione derivatives [89]. The IC_{50} values were identified in three different tumor cell lines and a highly potent antiproliferative compound **89** was confirmed (Fig. 7). With the introduction of an amino group on the para position of benzene ring, compound **89** showed the best antiproliferative activity against all four cell lines such as L1210, CEM, HeLa and HMEC-1 with IC_{50} values of 26 nM, 12 nM, 33 nM and 29 nM respectively. Hu *et al* designed and synthesized a series of 3-{[(9*H*-purin-6-yl) amino] methyl} pyridin-2(1*H*)-one derivatives [90] as tubulin polymerization inhibitors. The SAR analysis revealed that purine *N*-9 replaced by small

fatty groups showed good antiproliferative activity. The IC_{50} values of the optimal compound **90** (Fig. 7) in CT26, SW620 and HCT116 cells were 57 nM, 40 nM, 21 nM respectively. Shao *et al* designed and synthesized a series of novel paclitaxel benzofuran derivatives as inhibitors of microtubule polymerization [91] and evaluated their biological activities. Among them, compound **91** (Fig. 7) showed potent antiproliferative activity, which was significantly better than the positive control drug paclitaxel and had a better IC_{50} value of 0.58 μM against HT116 cells. Wang's research group synthesized a series of naphthalene cyclic benzophenone derivatives as tubulin polymerization inhibitors aiming at colchicine binding sites [92]. Most of the derivatives revealed good to moderate cytotoxicity against the MCF-7 cell line. Among them, the IC_{50} value of the optimal compound **92** (Fig. 7) on MCF-7 cells was 1.47 μM. The preliminary SAR analysis indicated that there was almost no antiproliferative activity without substitution on the benzene ring, and the single substituent group did not significantly improve the effect, while the 3-hydroxy-4-methoxy group on the benzene ring exhibited a much more important role in improving activity. Some novel derivatives of the 2,7-diaryl pyrazolo[1,5-a]pyrimidine series were revealed by Liu's team as inhibitors of microtubule polymerisation [93].

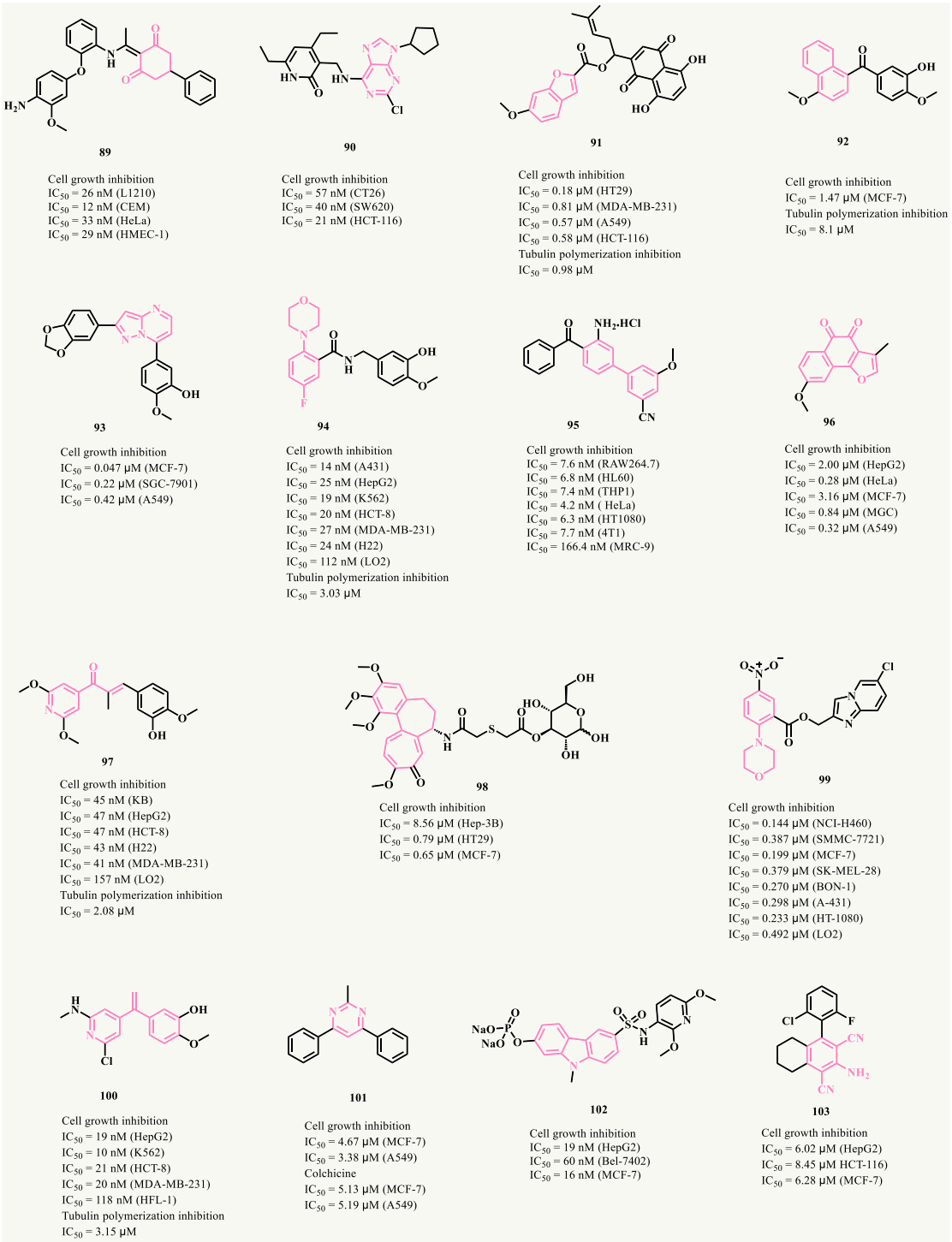

Fig. 7 Chemical structures of compounds **89**~**103**

According to SAR analysis, the substitution of electron-withdrawing groups or large steric hindrance groups on the benzene ring connected at the 7-position of pyrimidine will lead to the loss of activity while amino and hydroxyl groups show good activity. The nitrogen and oxygen atoms at this position are able to interact with the active sites in the pocket in a variety of ways, which lead to a complete loss of activity if there are no substitutions. The antiproliferative activity *in vitro* of the optimal compound **93** (Fig. 7) against three cancer cell lines (MCF-7, SGC-7901 and A549) was

assessed. Among them, compound **93** had the strongest antiproliferative activity against MCF-7 with the IC_{50} value of 47 nM, which destroyed its microtubule structure and blocked the cell cycle in G2/M phase. As revealed from another report of our research group, Zhu *et al* designed and synthesized a series of novel *N*-benzylbenzamide derivatives as inhibitors of microtubule protein polymerization [94]. As show in Fig. 8, when the R^2 group in the B ring was methoxy, the activity was significantly improved while the substitution of hydroxyl or halogen group would lead to the loss of activity and the substitution of R^3 hydrogen atom also led to the loss of activity. When R^1 was substituted by hydroxyl, the cytotoxicity was optimal, and the stability of the amide as the connecting chain between A and B rings might be better. When piperidine ring was introduced into the R^4, the activity was about four times higher than that of the morpholine ring, and when the oxygen atom in the morpholine ring was replaced with sulfur, the activity was slightly reduced, while the introduction of a nitrogen atom or sulfonyl group led to the loss of activity. There would be good antiproliferative activity while R^5 was replaced by halogen or methoxy, trifluoromethyl, etc or with no substituent. Among them, the fluorine atom produced the optimal effect. Compound **94** showed significant antiproliferative activity against a variety of cancer cell lines with an IC_{50} value for A431 cells at only 14 nM. Mechanistic studies showed that compound **94** bound to colchicine binding sites and displayed potent anti-vascular activity.

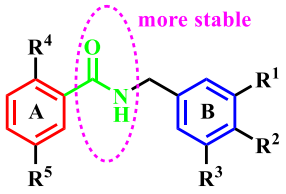

Fig. 8 The comprehensive SARs of *N*-benzylbenzamide derivatives

Through the modification of asymmetric diaryl compounds, Cheng's research group found a new compound dxy-1-175 based on the colchicine binding site of tubulin [95]. According to the lead compound, a series of novel 4-benzoyl biphenyl derivatives were designed and synthesized. In the attempt to replace and modify the three benzene rings, it was revealed that the 2-amino substitution of the middle benzene ring can significantly improve the antiproliferative activity, and the non-substitution of the left benzene ring can be better embedded in the efficacy pocket. Compound **95** (Fig. 7) exhibited the most potent antiproliferative activity. Compared with colchicine and dxy-1-175, compound **95** can effectively overcome multidrug resistance, and the RI index of KB-VCR, KB-V1 and K562-ADR was ≤ 1 (colchicine: 16-64; dxy-1-175: 0.8-2.2). The natural product tanshinone certainly has antitumor effects, but its poor antiproliferative activity and water solubility limited further clinical applications [96-97]. Based on the existing challenges, Huang *et al* optimized the structure of tanshinone, consequently, novel tanshinone derivatives were designed and synthesized [98]. The optimal compound **96** (Fig. 7) could bind to the colchicine site of tubulin, inhibited tubulin assembly and collapsed the microtubule network. Xu *et al* designed and

synthesized several kinds of novel pyridine-chalcone derivatives as potential anti-microtubule compounds [99]. Among them, the optimal compound **97** (Fig. 7) was sensitive to K562 cancer cell line and showed the most potent antiproliferative activity. The IC_{50} value was 23 nM. Based on the strategy that glucose conjugates can be selectively moved to tumor cells via glucose transport proteins [100-103], Wang's group designed a series of novel colchicine glycoconjugates as inhibitors of microtubule polymerisation [104]. Among these, compound **98** (Fig. 7) showed potent antiproliferative activity against high GLUT1 expressing cells (HT-29 and MCF-7), while activity was significantly decreased against low GLUT1 expressing cells. Zheng *et al* found a new compound **99** with increased water solubility based on the previously reported tubulin inhibitor IMB5046 (Fig. 7) [105]. With the antiproliferative activity assay, IC_{50} value of compound **99** was 0.144 μM in NCI-H460 cells and the water solubility was increased four-fold in the physiological environment with pH = 7.4, indicating that this may improve the *in vivo* absorption rate and bioavailability of drugs. Based on the lead compound iso-combretastatin A-4, Shuai *et al* designed and synthesized a series of novel isocomretapyridines as colchicine polymerization inhibitors [106]. The IC_{50} values of the optimal compound **100** (Fig. 7) against K562, HepG2, HCT-8, MDA-MB-231 and HFL-1 cells were 10 nM, 19 nM, 21 nM, 20 nM, 118 nM, respectively and compound **100** was most sensitive to K562 cells. Through SAR analysis, the double bond on the leakage chain was crucial for enhancing antiproliferative activity, and the 3-hydroxy-4-methoxyphenyl moiety was mostly favored. The 2-chloro-6-methylaminopyridine group was the most favorable. Further mechanistic studies showed that compound **100** disrupted microtubule networks, arrested cell cycle at G2/M phase, induced apoptosis and depolarized mitochondria of K562 cells in a dose-dependent manner. Bhupinder Kumar *et al* designed and synthesized a series of pyrimidinephenyl derivatives as tubulin polymerization inhibitors by optimizing combretastatin A-4 and evaluated for antiproliferative activities against MCF-7 and A549 cell lines [107]. And the IC_{50} values of optimal compound **101** (Fig. 7) were 4.67 μM and 3.38 μM on MCF-7 and A549 cell lines respectively, which were more effective than colchicine control (5.13 μM and 5.19 μM respectively). Further mechanistic studies exhibited that compound **101** inhibited the cell proliferation of cancer cells by altering the mitochondrial membrane potential which led to the leakage of cytochrome-c into the cytoplasm triggering intrinsic apoptotic pathway. Liu *et al* reported new carbazole sulfonamide derivatives [108]. The IC_{50} values were identified in three different cancer cell lines and a highly potent antiproliferative compound **102** was confirmed (Fig. 7). The representative compound **102** showed the best antiproliferative activity against three cell lines such as HepG2, Bel-7402 and MCF-7 with IC_{50} values of 19 nM, 60 nM and 16 nM respectively. Mennatallah *et al* designed and synthesized a series of novel 2-amino-1,4,5,6,7,8-hexahydroquinoline-3-carbonitriles derivatives as inhibitors of microtubule polymerization [109] and evaluated their biological activities. Among them, compound **103** (Fig. 7) showed moderate antiproliferative activity against HepG2, HCT-116 and MCF-7 cells *in vitro*, with IC_{50} values ranging from 6.02 ~ 8.45 μM.

Conclusion

In summary, this review represents only a partial knowledge of the current CBSIs, to provide a foundation for the design of the next generation of tubulin polymerization inhibitors. The dynamic stability and fragility of microtubules, as dynamic part of structures in cells, make them susceptible to interference by internal and external factors, and subtle disturbances to the dynamic process can lead to cell cycle arrest and further apoptosis. The tremendous roles of microtubules in cell division have made it a fascinating target for anti-cancer drugs, and scientists have developed a variety of inhibitors targeting microtubule-associated proteins, leading to the design of many high potential MTAs. Especially the development of CBSIs has attracted the interest of researchers worldwide compared to other binding sites, and some lead compounds are already in different phases of clinical trials. So far, CBSIs have critical limitations in clinical application generally due to highly toxicity. However, CBSIs will go further with some new strategies. For example, the rapidly developing antibody-drug conjugates (ADC) strategy enables compound molecules bounding to targeted antigens on the surface of tumor cells through antibodies, and tumor cells will internalize ADC molecules and release active products in lysosomes, which has the advantages of high targeting and specificity, low toxicity and side effects for tumor clinical treatment. In addition, the clinical application potential of tubulin inhibitors also could be improved by bioorthogonal strategy which is temporarily blocking the active compounds through transporting them to the tumor area and releasing the active product by catalytic cleavage. The analysis of the binding regions of the developed CBSIs and the modeling of the compounds' pharmacophore by molecular simulation technology have helped to identify more potent CBSIs with novel structures. There are several representative backbones for CBSIs, for example, the SAR suggested that the structures of the 3,4,5-trimethoxybenzene ring, quinazoline and indole ring play a key role in antiproliferative activity in the structural domain of CBSIs. Some compounds possessed structures of 3,4,5-trimethoxyphenyl, with triazole ring linkages, and these are all pivotal components for their antiproliferative activity. These are important pharmacodynamic fragments of highly active microtubule protein inhibitors, and further studies on their mechanism of action and structural relationship will provide a more scientific basis for further rational drug design.

Future perspective

Update CBSIs researches have yielded fruitful results, however, the development of drug resistance and toxicities still restricts the applications of CBSIs in the clinic. New strategies to overcome these limitations are urgently needed. It is the ultimate goal of every researcher to further strengthen *in vivo* pharmacokinetics and modification studies of CBSIs, and to improve stability, water solubility and other physicochemical properties of CBSIs. The classical lead compound CA-4 was terminated in clinical trial due to its instability after administration *in vivo*, which easily caused isomer inversion leading to *E*-type isomer to reduce the antiproliferative activity. Therefore, many research groups optimized CA-4 scaffold by introducing rigid groups in the linkage to prevent the

configuration reversal. Properly introducing hydrophilic groups such as phosphate ester to improve the water solubility of tubulin inhibitors and designing ADCs or bioorthogonal strategy prodrugs to improve targeted capacity and reduce toxicity of compounds were also performed. Meanwhile, more alternatives that possess similar characters of established privileged structures remain to be further validated. Some prodrug forms used to improve aqueous solubility and PK profiles could continue to be investigated. Furthermore, with the advances in innovative strategies of drug discovery, it is feasible to develop novel dual-target tubulin inhibitors [110-112] to improve therapeutic effects and overcome drug resistance.

The druglikeness optimization of the next generation of target tubulin inhibitors may involve how to make use of optimizing the physicochemical properties and delivery system. We are especially concerned that the bioorthogonal cleavage would be a new trend in the target tubulin inhibitors development. We believe that new therapeutic strategies and agents are emerging, both for the treatment of cancer and for other diseases with the advancement of knowledge on the structure of tubulin, the regulation of microtubule dynamics and their deregulation in pathological processes. As such, by rationalizing the design of colchicine binding site inhibitors, it is hoped that more novel CBSIs with high efficiency, low toxicity, high bioavailability and anti-multidrug resistance will be discovered.

Executive Summary

• Microtubules, a critical component of eukaryotic cells, are hollow cylinders formed by the polymerization of α-tubulin and β-tubulin heterodimer playing a critical role in the formation of the cell cytoskeleton, maintenance of cell morphology, signal transduction and mitosis.

• Microtubules are considered as a major target to prevent the proliferation of tumor cells. Microtubule-targeted agents (MTAs) have become increasingly effective anticancer drugs.

• Colchicine binding site inhibitors (CBSIs) are more easily modified and have a potent anti-proliferative effect on multidrug resistant (MDR) cancer cells.

• Representative structures of CBSIs are discussed including quinazoline derivatives, indole analogues, CA-4 analogues, 3,4,5-trimethoxybenzene ring and triazole ring linkages, etc which showed effective antiproliferative activity against different kinds of cancer cell lines and multidrug resistant (MDR) cancer cell lines.

Financial & competing interests disclosure

This work was supported by the grant from the National Natural Science Foundation of China (no 82173679）. The authors have no other relevant affiliations or financial involvement with any organization or entity with a financial interest in or financial conflict with the subject matter or materials discussed in the manuscript apart from those disclosed. No writing assistance was utilized in the production of this manuscript.

References.

Papers of special note have been highlighted as: • of interest; •• of considerable interest

1. Siegel RL, Miller KD, Fuchs HE, Jemal A. Cancer Statistics. *CA. Cancer. J. Clin*. 72(1), 7–33 (2022).

• A comprehensive and authoritative statistics which exhibited the severity situation of tumor worldwide.

2. Sung H, Ferlay J, Siegel RL *et al*. Global Cancer Statistics 2020: GLOBOCAN estimates of incidence and mortality worldwide for 36 cancers in 185 countries. *CA. Cancer. J. Clin.* 71(3), 209-249 (2021).

3. Howard J, Hyman AA. Dynamics and mechanics of the microtubule plus end. *Nature*. 17,422(6933), 753–8 (2003).

4. Jordan MA, Wilson L. Microtubules as a target for anticancer drugs. *Nat. Rev. Cancer*. 4(4), 253–65 (2004).

5. Downing KH, Nogales E. Tubulin structure: insights into microtubule properties and functions. *Curr. Opin. Struct. Biol.* 8(6), 785–91 (1999).

6. Ferrara R, Pilotto S, Peretti U *et al*. Tubulin inhibitors in non-small cell lung cancer: looking back and forward. *Expert. Opin. Pharmacother*. 17(8), 1113–29 (2016).

7. Chaudhary V, Venghateri JB, Dhaked HPS, Bhoyar AS, Guchhait SK, Panda D. Novel combretastatin-2-aminoimidazole analogues as potent tubulin assembly inhibitors: exploration of unique pharmacophoric impact of bridging skeleton and aryl moiety. *J. Med. Chem*. 59(7), 3439–51 (2016).

8. Steinmetz MO, Prota AE. Microtubule-targeting agents: strategies to hijack the cytoskeleton. *Trends. Cell. Biol.* 28(10), 776–792 (2018).

9. Dumontet C, Jordan MA. Microtubule-binding agents: a dynamic field of cancer therapeutics. *Nat. Rev. Drug Discov*. 9(10), 790–803 (2010).

10. Baytas SN. Recent advances in Combretastatin A-4 inspired inhibitors of tubulin polymerization: an update. *Curr Med Chem*. 29(20), 3557–3585 (2022).

11. Borisy G, Heald R, Howard J, Janke C, Musacchio A, Nogales E. Microtubules: 50 years on from the discovery of tubulin. *Nat. Rev. Mol. Cell. Biol*. 17(5), 322–8 (2016).

12. Ravelli RBG, Gigant B, Curmi PA, Jourdain I, Lachkar S, Sobel A, Knossow M. Insight into tubulin regulation from a complex with colchicine and a stathmin-like domain. *Nature*. 11, 428(6979), 198–202 (2004).

13. Chinen T, Liu P, Shiodaet S *et al*. The γ-tubulin-specific inhibitor gatastatin reveals temporal requirements of microtubule nucleation during the cell cycle. *Nat. Commun.* 6, 8722 (2015).

14. Bai R, Covell DG, Pei XF *et al*. Mapping the binding site of colchicinoids on beta-tubulin. 2-Chloroacetyl-2-demethylthiocolchicine covalently reacts predominantly with cysteine 239 and secondarily with cysteine 354. *J. Biol. Chem.* 275 (51), 40443–52 (2000).

15. Kuppens IELM, Witteveen PO, Schot M *et al*. Phase I dose-finding and pharmacokinetic trial of orally administered indibulin (D-24851) to patients with solid tumors. *Invest. New Drugs.* 25(3), 227–35 (2007).

16. Patterson DM, Zweifel M, Middleton MR *et al*. Phase I clinical and pharmacokinetic evaluation of the vascular-disrupting agent OXi4503 in patients with advanced solid tumors. *Clin. Cancer Res.* 18(5), 1415–25 (2012).

17. Liu P, Qin Y, Wu L *et al*. A phase I clinical trial assessing the safety and tolerability of combretastatin A4 phosphate injections. *Anticancer Drugs.* 25(4), 462–71 (2014).

• CA4P successfully entered clinical trial stage and the result showed it was generally well tolerated and Ninety-five percent of adverse events were mild.

18. Fox E, Maris JM, Widemann BC *et al*. A phase 1 study of ABT -751, an orally bioavailable tubulin inhibitor, administered daily for 7 days every 21 days in pediatric patients with solid tumors. *Clin. Cancer Res.* 14(4), 1111–5 (2008).

19. Hawash M. Recent advances of tubulin inhibitors targeting the colchicine binding site for cancer therapy. *Biomolecules.* 12(12), 1843 (2022).

20. Guggilapu SD, Lalita G Reddy TS *et al*. Synthesis of C5-tethered indolyl-3-glyoxylamide derivatives as tubulin polymerization inhibitors. *Eur. J. Med. Chem.* 128, 1–12 (2017).

21. Mirzaei H, Shokrzadeh M, Modanloo M, Ziar A, Riazi GH, Emami S. New indole-based chalconoids as tubulin-targeting anti-proliferative agents. *Bioorg. Chem.* 75, 86–98 (2017).

22. Wang G, Peng Z, Li Y. Synthesis, anticancer activity and molecular modeling studies of novel chalcone derivatives containing indole and naphthalene moieties as tubulin polymerization inhibitors. *Chem. Pharm. Bull*. 67(7), 725–728 (2019).

23. Kode J, Kovvuri J, Nagaraju B *et al*. Synthesis, biological evaluation, and molecular docking analysis of phenstatin based indole linked chalcones as anticancer agents and tubulin polymerization inhibitors. *Bioorg. Chem*. 105, 104447 (2020).

24. Zhu H, Sun H, Liu Y *et al*. Design, synthesis and biological evaluation of vinyl selenone derivatives as novel microtubule polymerization inhibitors. *Eur. J. Med. Chem*. 207, 112716 (2020).

•• Provided a special and privileged scaffold of tubulin inhibitor.

25. Ramya PVS, Angapelly S, Guntuku L *et al*. Synthesis and biological evaluation of curcumin inspired indole analogues as tubulin polymerization inhibitors. *Eur. J. Med. Chem.* 127, 100–114 (2017).

26. Arnst KE, Wang Y, Hwang DJ *et al*. A potent, metabolically stable tubulin inhibitor targets the colchicine binding site and overcomes taxane resistance. *Cancer Res.* 78(1), 265–277 (2018).

27. Li W, Sun H, Xu F *et al*. Synthesis, molecular properties prediction and biological evaluation of indole-vinyl sulfone derivatives as novel tubulin polymerization inhibitors targeting the colchicine binding site.
Bioorg. Chem. 85, 49–59 (2019).

28. Regina GL, Bai R, Coluccia A *et al*. New 6- and 7-heterocyclyl-1H-indole derivatives as potent tubulin assembly and cancer cell growth inhibitors. *Eur. J. Med. Chem.* 152, 283–297 (2018).

29. Sigalapalli DK, Pooladanda V, Singh P *et al*. Discovery of certain benzyl/phenethyl thiazolidinone-indole hybrids as potential anti-proliferative agents: Synthesis, molecular modeling and tubulin polymerization inhibition study. *Bioorg. Chem*. 92, 103188 (2019).

30. Wang Q, Arnst KE, Wang Y *et al*. Structure-guided design, synthesis, and biological evaluation of (2-(1h-indol-3-yl)-1h-imidazol-4-yl)(3,4,5-trimethoxyphenyl) methanone (abi-231) analogues targeting the colchicine binding site in tubulin. *J. Med. Chem*. 62(14), 6734–6750 (2019).

31. Cui Y, Ma C, Zhang C, Tang L, Liu Z. The discovery of novel indazole derivatives as tubulin colchicine site binding agents that displayed potent antitumor activity both *in vitro* and *in vivo*. *Eur. J. Med. Chem.* 187, 111968 (2020).

32. Romagnoli R, Prencipe F, Oliva P *et al*. Design, synthesis and biological evaluation of 2-alkoxycarbonyl-3-anilinoindoles as a new class of potent inhibitors of tubulin polymerization. *Bioorg. Chem*. 97, 103665 (2020).

33. Naaz F, Ahmad F, Lone BA *et al*. Design and synthesis of newer 1,3,4-oxadiazole and 1,2,4-triazole based Topsentin analogues as anti-proliferative agent targeting tubulin. *Bioorg. Chem*. 95, 103519 (2020).

34. Li G, Wang Y, Li L *et al*. Design, synthesis, and bioevaluation of pyrazolo[1,5-a]pyrimidine derivatives as tubulin polymerization inhibitors targeting the colchicine binding site with potent anticancer activities. *Eur. J. Med. Chem*. 202, 112519 (2020).

35. Wu C, Wu J, Hu Y*et al*. Design, synthesis and biological evaluation of indole-based[1,2,4]triazolo[4,3-*a*] pyridine derivatives as novel microtubule polymerization inhibitors. *Eur. J. Med. Chem*. 223, 113629 (2021).

36. Pecnard S, Provot O, Levaique H *Et al*. Cyclic bridged analogs of isoCA-4: Design, synthesis and biological evaluation. *Eur. J. Med. Chem*. 209, 112873 (2021).

37. Wang G, He M, Liu W, Fan M, Li Y, Peng Z. Design, synthesis and biological evaluation of novel 2-phenyl-4,5,6,7-tetrahydro-1H-indole derivatives as potential anticancer agents and tubulin polymerization inhibitors. *Arabian Journal of Chemistry*. 15, 103504 (2022).

38. Saruengkhanphasit R, Butkinaree C, Ornnork N *et al*. Identification of new 3-phenyl-1H-indole-2-carbohydrazide derivatives and their structure–activity relationships as potent tubulin inhibitors and anticancer agents: A combined in silico, *in vitro* and synthetic study. *Bioorg. Chem*. 110, 104795 (2021).

39. Hawash M, Kahraman DC, Olgac A *et al*. Design and synthesis of novel substituted indole-acrylamide derivatives and evaluation of their anti-cancer activity as potential tubulin-targeting agents. *J Mol Struct*. 1254, 132345 (2022).

40. Thanaussavadate B, Ngiwsara L, Lirdprapamongkol K, Svasti J, Chuawong P. A synthetic 2,3-diarylindole induces microtubule destabilization and G2/M cell cycle arrest in lung cancer cells. *Bioorg Med Chem Lett*. 30(1), 126777 (2020).

41. Wang SY, Liu X, Meng LW *et al*. Discovery of indoline derivatives as anticancer agents via inhibition of tubulin polymerization. *Bioorg Med Chem Lett*. 43, 128095 (2021).

42. Diao PC, Jian XE, Chen P *et al*. Design, synthesis and biological evaluation of novel indole-based oxalamide and aminoacetamide derivatives as tubulin polymerization inhibitors. *Bioorg Med Chem Lett*. 30(2), 126816 (2020).

43. Brel VK, Artyushin OI, Chuprov-Netochin RN *et al*. Synthesis and biological evaluation of indolylglyoxylamide bisphosphonates, antimitotic microtubule-targeting derivatives of indibulin with improved aqueous solubility. *Bioorg Med Chem Lett*. 30(23), 127635 (2020).

44. Chen P, Zhuang Y, Diao P *et al*. Synthesis, biological evaluation, and molecular docking investigation of 3-amidoindoles as potent tubulin polymerization inhibitors. *Eur. J. Med. Chem*. 162, 525–533 (2019).

45. Zhai M, Liu S, Gao M *et al*. 3,5-Diaryl-1H-pyrazolo[3,4-b]pyridines as potent tubulin polymerization inhibitors: Rational design, synthesis and biological evaluation. *Eur. J. Med. Chem*. 168, 426–435 (2019).

46. Yin Y, Lian Bao, Xia Y, Shao Y, Kong L. Design, synthesis and biological evaluation of resveratrol-cinnamoyl derivates as tubulin polymerization inhibitors targeting the colchicine binding site. *Bioorg. Chem.* 93, 103319 (2019).

47. Jiang J, Zhang H, Wang C *et al*. 1-Phenyl-dihydrobenzoindazoles as novel colchicine site inhibitors: Structural basis and antitumor efficacy. *Eur. J. Med. Chem.* 177, 448–456 (2019).

48. Chen H, Deng S, Wang Y *et al*. Structure-activity relationship study of novel 6-aryl-2-benzoylpyridines as tubulin polymerization inhibitors with potent antiproliferative properties. *J. Med. Chem*. 63(2), 827–846 (2020).

•• The optimal compound based on the lead compound ABI-274 significantly induced tumor necrosis, and apoptosis without observed toxicity.

49. Li L, Quan D, Chen J *et al*. Design, synthesis, and biological evaluation of 1-substituted -2-aryl imidazoles targeting tubulin polymerization as potential anticancer agents. *Eur. J. Med. Chem*. 184, 111732 (2019).

50. Zhao W, He L, Xiang T, Tang Y. Discover 4b-NH-(6-aminoindole)-4-desoxy-podophyllotoxin with nanomolar-potency antitumor activity by improving the tubulin binding affinity on the basis of a potential binding site nearby colchicine domain. *Eur. J. Med. Chem*. 170, 73–86 (2019).

51. Song J, Gao Q, Wu B *et al*. Discovery of tertiary amide derivatives incorporating benzothiazole moiety as anti-gastric cancer agents *in vitro* via inhibiting tubulin polymerization and activating the Hippo signaling pathway. *Eur. J. Med. Chem*. 203, 112618 (2020).

52. Sun Y, Song J, Kong L *et al*. Design, synthesis and evaluation of novel bis-substituted aromatic amide dithiocarbamate derivatives as colchicine site tubulin polymerization inhibitors with potent anticancer activities. *Eur. J. Med. Chem*. 229, 114069 (2022).

53. Liu X, Pang X, Liu Y *et al*. Discovery of novel diarylamide n-containing heterocyclic derivatives as new tubulin polymerization inhibitors with anti-cancer activity. *Molecules*. 26(13), 4047 (2021).

54. Yang B, Zhou J, Wang F, Hu X, Shi Y. Pyrazoline derivatives as tubulin polymerization inhibitors with one hit for vascular endothelial growth factor receptor 2 inhibition. *Bioorg. Chem*. 114, 105134 (2021).

55. Ren Y, Wang Y, Li G *et al*. Discovery of novel benzimidazole and indazole analogues as tubulin polymerization inhibitors with potent anticancer activities. *J. Med. Chem*. 64, 4498–4515 (2021).

56. Chen H, Deng S, Albadari N *et al*. Design, synthesis, and biological evaluation of stable colchicine binding site tubulin inhibitors 6-aryl-2-benzoyl-pyridines as potential anticancer agents. *J. Med. Chem*. 64(16), 12049–12074 (2021).

57. Yan X, Leng J, Chen T, Zhao Y, Kong L, Yin Y. Design, synthesis, and biological evaluation of novel diphenylamine derivatives as tubulin polymerization inhibitors targeting the colchicine binding site. *Eur. J. Med. Chem*. 237, 114372 (2022).

58. Li W, Shuai W, Xu F *et al*. Discovery of novel 4-arylisochromenes as anticancer agents inhibiting tubulin polymerization. *ACS Med Chem Lett*. 9(10), 974–979 (2018).

•• The highlight is the lead compound was extracted from nature peel of plant and optimized to obtain the optimal compound and exhibited potent antiproliferative effect against different cancer cell lines.

59. Ansari M, Shokrzadeh M, Karima S *et al*. New thiazole-2(3H)-thiones containing 4-(3,4,5-trimethoxyphenyl) moiety as anticancer agents. *Eur. J. Med. Chem*. 185, 111784 (2020).

60. He JP, Zhang M, Tang L *et al.* Synthesis, biological evaluation, and molecular docking of arylpyridines as antiproliferative agent targeting tubulin. *ACS Med. Chem. Lett*. 11(8), 1611–1619 (2020).

61. Lai Q, Wang Y, Wang R *et al.* Design, synthesis and biological evaluation of a novel tubulin inhibitor 7a3 targeting the colchicine binding site. *Eur. J. Med. Chem*. 156, 162–179 (2020).

62. Hawash M, Qaoud MT, Jaradat N *et al.* Anticancer activity of thiophene carboxamide derivatives as CA-4 biomimetics: synthesis, biological potency, 3D spheroid model, and molecular dynamics simulation. *Biomimetics*. 7(4), 247 (2022).

63. Xu Q, Bao K, Sun M *et al*. Design, synthesis and structureactivity relationship of 3,6-diaryl-7H-[1,2,4]triazolo[3,4-b][1,3,4]thiadiazines as novel tubulin inhibitors. *Sci Rep*. 7(1), 11997 (2017).

64. Fu D, Li P, Wu B, Cui X, Zhao C, Zhang S. Molecular diversity of trimethoxyphenyl-1,2,3-triazole hybrids as novel colchicine site tubulin polymerization inhibitors. *Eur. J. Med. Chem*. 165, 309–322 (2019).

65. Qi Z, Hao S, Tian H, Bian H, Hui L, Chen S. Synthesis and biological evaluation of 1-(benzofuran-3-yl)-4-(3,4,5-tr-imethoxyphenyl)-1H-1,2,3-triazole derivatives as tubulin polymerization inhibitors. *Bioorg. Chem*. 94, 103392 (2020).

66. Mustafa M, Anwar S, Elgamal F, Ahmed ER, Aly OM. Potent combretastatin A-4 analogs containing 1,2,4-triazole: Synthesis, antiproliferative, anti-tubulin activity, and docking study. *Eur. J. Med. Chem*. 183, 111697 (2019).

67. Ansaria M, Shokrzadeh M, Karima S *et al*. Design, synthesis and biological evaluation of flexible and rigid analogs of 4H-1,2,4-triazoles bearing 3,4,5-trimethoxyphenyl moiety as new antiproliferative agents. *Bioorg. Chem*. 93, 103300 (2019).

68. Wang C, Li Y, Liu T *et al*. Design, synthesis and evaluation of antiproliferative and antitubulin activities of 5-methyl-4-aryl-3-(4-arylpiperazine-1-carbonyl)-4H-1,2,4-triazoles. *Bioorg. Chem*. 104, 103909 (2020).

69. Hua S, Chen F, Wang X, Gou S. Dual-functional conjugates improving cancer immunochemotherapy by inhibiting tubulin polymerization and indoleamine-2,3-dioxygenase. *Eur. J. Med. Chem*. 189, 112041 (2020).

• The optimal compound composed of combretastatin A-4 and (D)-1-methyltryptophan showed effective antitumor activity. The conjugates revealed potential perspective in tubulin inhibitors.

70. Yang F, Jian X, Diao P, Huo X, You W, Zhao P. Synthesis, and biological evaluation of 3,6-diaryl-[1,2,4]triazolo[4,3-a]pyridine analogues as new potent tubulin polymerization inhibitors. *Eur. J. Med. Chem*. 204, 112625 (2020).

71. Huo X, Jian X, Yang J *et al*. Discovery of highly potent tubulin polymerization inhibitors: Design, synthesis, and structure-activity relationships of novel 2,7-diaryl-[1,2,4]triazolo[1,5-a]pyrimidines. *Eur. J. Med. Chem*. 220, 113449 (2021).

72. Eissa IH, Dahab MA, Ibrahimet MK *et al*. Design and discovery of new antiproliferative 1,2,4-triazin-3(2H)-ones as tubulin polymerization inhibitors targeting colchicine binding site. *Bioorg. Chem*. 112, 104965 (2021).

73. Wu M, Man R, Liao Y, Zhu H, Zhou Z. Discovery of novel indole-1,2,4-triazole derivatives as tubulin polymerization inhibitors. *Drug. Dev Res*. 82(7), 1008–1020 (2021).

74. Mohamed HS, Amin NH, El-Saadi MT, Abdel-Rahman HM. Design, synthesis, biological assessment, and in-Silico studies of 1,2,4-triazolo[1,5-a]pyrimidine derivatives as tubulin polymerization inhibitors. *Bioorg. Chem*. 121, 105687 (2022).

75. Ma W, Chen P, Huo X *et al*. Development of triazolothiadiazine derivatives as highly potent tubulin polymerization inhibitors: Structure-activity relationship, in vitro and in vivo study. *Eur. J. Med. Chem*. 208, 112847 (2020).

76. Yang F, Yu LZ, Diao PC *et al*. Novel [1,2,4]triazolo[1,5-a]pyrimidine derivatives as potent antitubulin agents: Design, multicomponent synthesis and antiproliferative activities. *Bioorg. Chem*. 92, 103260 (2019).

77. Yang F, He CP, Diao PC, Hong KH, Rao JJ, Zhao PL. Discovery and optimization of 3,4,5-trimethoxyphenyl substituted triazolylthioacetamides as potent tubulin polymerization inhibitors. *Bioorg Med Chem Lett*. 29(1), 22–27 (2019).

78. Mustafa M, Abdelhamid D, Abdelhafez EMN, Ibrahim MAA, Gamal-Eldeen AM, Aly OM. Synthesis, antiproliferative, anti-tubulin activity, and docking study of new 1,2,4-triazoles as potential combretastatin analogues. *Eur. J. Med. Chem*. 141, 293–305 (2017).

79. Li W, Yin Y, Shuai W *et al*. Discovery of novel quinazolines as potential anti-tubulin agents occupying three zones of colchicine domain. *Bioorg. Chem*. 83, 380–390 (2019).

80. Liang T, Zhou X, Lu L *et al*. Structure-activity relationships and antiproliferative effects of 1,2,3,4-4H-quinoxaline derivatives as tubulin polymerization inhibitors. *Bioorg. Chem*. 110, 104793 (2021).

81. Ren Y, Ruan Y, Cheng B *et al*. Design, synthesis and biological evaluation of novel acridine and quinoline derivatives as tubulin polymerization inhibitors with anticancer activities. *Bioorg. Med. Chem*. 46, 116376 (2021).

82. Wang K, Zhong H, Li N *et al*. Discovery of novel anti-breast-cancer inhibitors by synergistically antagonizing microtubule polymerization and aryl hydrocarbon receptor expression. *J. Med. Chem*. 64(17), 12964–12977 (2021).

83. Li W, Shuai W, Sun H *et al*. Design, synthesis and biological evaluation of quinoline-indole derivatives as anti-tubulin agents targeting the colchicine binding site. *Eur. J. Med. Chem*. 163, 428–442 (2019).

84. Elhemely MA, Belgath AA, El-Sayed S *et al*. SAR of novel 3-arylisoquinolinones: meta-substitution on the aryl ring dramatically enhances antiproliferative activity through binding to microtubules. *J. Med. Chem*. 65(6), 4783–4797 (2022).

85. Li W, Xu F, Shuai W *et al*. Discovery of novel quinoline-chalcone derivatives as potent antitumor agents with microtubule polymerization inhibitory activity. *J. Med. Chem*. 62(2), 993–1013 (2019).

86. Mirzaei S, Eisvand F, Hadizadeh F, Mosaffa F, Ghasemi A, Ghodsi R. Design, synthesis and biological evaluation of novel 5,6,7-trimethoxy-N-aryl-2-styrylquinolin-4-amines as potential anticancer agents and tubulin polymerization inhibitors. *Bioorg. Chem*. 98, 103711 (2020).
87. Rehulka J, Vychodilova K, Krejcí P *et al*. Fluorinated derivatives of 2-phenyl-3-hydroxy-4(1H)-quinolinone as tubulin polymerization inhibitors. *Eur. J. Med. Chem*. 192, 112176 (2020).
88. Khelifi I, Naret T, Hamze A *et al*. N,N-bis-heteroaryl methylamines: Potent anti-mitotic and highly cytotoxic agents. *Eur. J. Med. Chem*. 168, 176–188 (2019).
89. Bueno O, Gargantilla M, Estévez-Gallegoet J *et al*. Diphenyl ether derivatives occupy the expanded binding site of cyclohexanedione compounds at the colchicine site in tubulin by movement of the αT5 loop. *Eur. J. Med. Chem*. 171, 195–208 (2019).
90. Hu X, Li L, Zhang Q *et al*. Design, synthesis and biological evaluation of a novel tubulin inhibitor SKLB0565 targeting the colchicine binding site. *Bioorg. Chem*. 97, 103695 (2020).
91. Shao Y, Yin Y, Lian B, Leng J, Xia Y, Kong L *et al*. Synthesis and biological evaluation of novel shikonin-benzo[b]furanderivatives as tubulin polymerization inhibitors targeting the colchicine binding site. *Eur. J. Med. Chem*. 190, 112105 (2020).
92. Wang G, Liu W, Tang J *et al*. Design, synthesis, and anticancer evaluation of benzophenone derivatives bearing naphthalene moiety as novel tubulin polymerization inhibitors. *Bioorg. Chem*. 104, 104265 (2020).
93. Liu R, Zhang S, Huang M *et al*. Design, synthesis and bioevaluation of 2,7-diaryl-pyrazolo[1,5-a] pyrimidines as tubulin polymerization inhibitors. *Bioorg. Chem*. 115, 105220 (2021).
94. Zhu H, Li W, Shuai W *et al*. Discovery of novel N-benzylbenzamide derivatives as tubulin polymerization inhibitors with potent antitumor activities. *Eur. J. Med. Chem*. 216, 113316 (2021).
95. Cheng B, Zhu G, Meng L, Wu G, Chen Q, Ma S. Identification and optimization of biphenyl derivatives as novel tubulin inhibitors targeting colchicine-binding site overcoming multidrug resistance. *Eur. J. Med. Chem*. 228, 113930 (2022).
96. Su C, Ming Q, Rahman K, Han T, Qin L. Salvia miltiorrhiza: Traditional medicinal uses, chemistry, and pharmacology. *Chin. J. Nat. Med*. 13(3), 163–82 (2015).
97. Zhang Y, Jiang P, Ye M, Kim S, Jiang C, Lü J. Tanshinones: sources, pharmacokinetics and anti-cancer activities. *Int. J. Mol. Sci*. 13(10), 13621–66 (2012).
98. Huang H, Yao Y, Hou G *et al*. Design, synthesis and biological evaluation of tanshinone IIA-based analogues: Potent inhibitors of microtubule formation and angiogenesis. *Eur. J. Med. Chem*. 224, 113708 (2021).
•• SAR provided detailed information and sparked to design potent tubulin inhibitors.
99. Xu F, Li W, Shuai W *et al*. Design, synthesis and biological evaluation of pyridine-chalcone derivatives as novel microtubule-destabilizing agents. *Eur. J. Med. Chem*. 173, 1–14 (2019).
100. Lin Y, Tungpradit R, Sinchaikul S *et al*. Targeting the delivery of glycan-based paclitaxel prodrugs to cancer cells via glucose transporters. *J. Med. Chem*. 51(23), 7428–41 (2008).
101. Calvaresi EC, Hergenrother PJ. Glucose conjugation for the specific targeting and treatment of cancer. *Chem. Sci*. 4(6), 2319–2333 (2013).
102. Liu P, Lu Y, Gao X *et al*. Highly water-soluble platinum (II) complexes as GLUT substrates for targeted therapy: improved anticancer efficacy and transportermediated cytotoxic properties. *Chem. Commun*. 49(24), 2421–3 (2013).
103. Han J, Gao X, Liu R *et al*. Design, synthesis of novel platinum (II) glycoconjugates, and evalution of their antitumor effects. *Chem Biol Drug Des*. 87(6), 867–77 (2016).
104. Wang Z, Liu R, Zhang X *et al*. Design, synthesis and biological evaluation of colchicine glycoconjugates as tubulin polymerization inhibitors. *Bioorg Med Chem*. 58, 116671 (2022).

105. Zheng Y, Dong Y, Si S, Zhen Y, Gong J. IMB5476, a novel microtubule inhibitor, induces mitotic catastrophe and overcomes multidrug resistance in tumors. *Eur. J. Pharmacol*. 919, 174802 (2022).

106. Shuai W, Li X, Li W *et al*. Design, synthesis and anticancer properties of isocombretapyridines as potent colchicine binding site inhibitors. *Eur. J. Med. Chem*. 197, 112308 (2020).

107. Kumar B, Sharma P, Gupta VP *et al*. Synthesis and biological evaluation of pyrimidine bridged combretastatin derivatives as potential anticancer agents and mechanistic studies. *Bioorg. Chem*. 78, 130–140 (2018).

108. Liu Y, Wu Y, Sun L, Gu Y, Hu L. Synthesis and structure-activity relationship study of water-soluble carbazole sulfonamide derivatives as new anticancer agents. *Eur. J. Med. Chem*. 191, 112181 (2020).

109. Shaheen MA, El-Emam AA, El-Gohary NS. 1,4,5,6,7,8-Hexahydroquinolines and 5,6,7,8-tetrahydronaphthalenes: A new class of antitumor agents targeting the colchicine binding site of tubulin. *Bioorg. Chem*. 99, 103831 (2020).

110. Shuai W, Wang G, Zhang Y *et al*. Recent progress on tubulin inhibitors with dual targeting capabilities for cancer therapy. *J. Med. Chem*. 64(12), 7963–7990 (2021).

•• Excellent review on the dual-target tubulin inhibitors.

111. Zhu H, Tan Y, He C *et al*. Discovery of a novel vascular disrupting agent inhibiting tubulin polymerization and HDACs with potent antitumor Effects. *J. Med. Chem*. 65(16), 11187–11213 (2022).

112. Fu D, Wang T. Discovery of dual tubulin-NEDDylation inhibitors with antiproliferative activity. *J Enzyme Inhib Med Chem*. 38(1), 166–175 (2022).